Inorganic Chemistry

ARTICLE

pubs.acs.org/IC

Stepwise Construction of Manganese−Chromium Carbonyl Chalcogenide Complexes: Synthesis, Electrochemical Properties, and Computational Studies

Minghuey Shieh,* Chia-Yeh Miu, Kuo-Chih Huang, Chung-Feng Lee, and Bao-Gun Chen

Department of Chemistry, National Taiwan Normal University, Taipei 116, Taiwan, Republic of China

Supporting Information

ABSTRACT: When trigonal-bipyramidal clusters, $[PPN][E_2Mn_3(CO)_9]$ (E = S, Se), were treated with $Cr(CO)_6$ and PPNCl in a molar ratio of 1:1:2 or 1:2:2 in 4 M KOH/MeCN/MeOH solutions, mono-$Cr(CO)_5$-incorporated HE_2Mn_3-complexes $[PPN]_2[HE_2Mn_3Cr(CO)_{14}]$ (E = S, $[PPN]_2$[**1a**]; Se, $[PPN]_2$[**1b**]), respectively, were formed. X-ray crystallographic analysis showed that **1a** and **1b** were isostructural and each displayed an E_2Mn_3 square-pyramidal core with one of the two basal E atoms externally coordinated with one $Cr(CO)_5$ group and one Mn−Mn bond bridged by one hydrogen atom. However, when the $TMBA^+$ salts for $[E_2Mn_3(CO)_9]^-$ were mixed with $Cr(CO)_6$ in a molar ratio of 1:1 in 4 M KOH/MeOH solutions and refluxed at 60 °C, mono-$Cr(CO)_3$-incorporated E_2Mn_3Cr octahedral clusters $[TMBA]_3[E_2Mn_3Cr(CO)_{12}]$ (E = S, $[TMBA]_3$[**2a**]; Se, $[TMBA]_3$[**2b**]), respectively, were obtained. Clusters **2a** and **2b** were isostructural, and each consisted of an octahedral E_2Mn_3Cr core, in which each Mn−Mn or Mn−Cr bond of the Mn_3Cr plane was semibridged by one carbonyl ligand. Clusters **1a** and **1b** (with [TMBA] salts) underwent metal core closure to form octahedral clusters **2a** and **2b** upon treatment with KOH/MeOH at 60 °C. In addition, **1a** and **1b** were found to undergo cluster expansion to form di-$Cr(CO)_5$-incorporated HE_2Mn_3-clusters $[HE_2Mn_3Cr_2(CO)_{19}]^{2-}$ (E = S, **3a**; Se, **3b**), respectively, upon the addition of 1 or 2 equiv of $Cr(CO)_6$ heated in refluxing CH_2Cl_2. Clusters **3a** and **3b** were structurally related to clusters **1a** and **1b**, but with the other bare E atom (E = S, **3a**; Se, **3b**) further externally coordinated with one $Cr(CO)_5$ group. The nature, cluster transformation, and electrochemical properties of the mixed manganese−chromium carbonyl sulfides and selenides were systematically discussed in terms of the chalcogen elements, the introduced chromium carbonyl group, and the metal skeleton with the aid of molecular calculations at the BP86 level of the density functional theory.

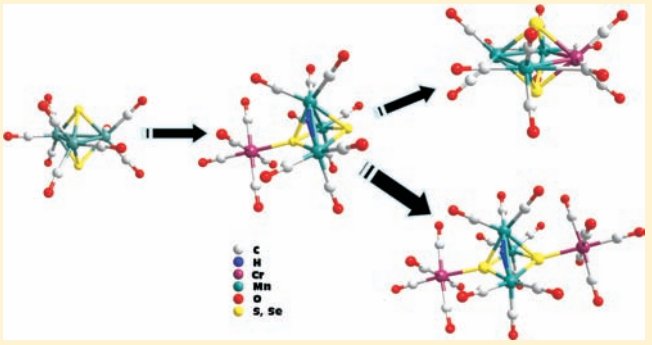

INTRODUCTION

Heterometallic cluster complexes represent a challenging area of synthetic chemistry because of their numerous applications in catalysis,[1,2] magnetism,[3,4] nanoscience,[5] and nanotechnology.[6] Although systematic syntheses of heteronuclear cluster complexes have advanced significantly during the past few years,[1c,7] rational stepwise cluster-growth processes, based on coupling reactions of suitable transition-metal species or the conversion of existing structural geometries to new ones, were few because of the lack of practical methodologies. In addition to the development of the fundamental chemistry among mixed-metal clusters, the exploration of the redox capacity of the high-nuclear homo- or heterometal carbonyl clusters is even more important because of their potential uses as molecular capacitors.[5b,8]

Whereas homonuclear iron[9−11] carbonyl chalcogenide clusters are well-developed, carbonylmanganese[9a−c,12−14] and carbonylchromium[9a−c,15−17] chalcogenide complexes have not been explored as much, and mixed manganese−chromium carbonyl chalcogenide complexes are even more rare.[18,19] Very recently, our group reported two mixed chromium−manganese selenide carbonyl complexes from the reaction of the paramagnetic species $[Se_2Cr_3(CO)_{10}]^{2-}$ with $Mn(CO)_5Br$ in acetone.[19c] However, the question of how to search for suitable building blocks for step-by-step construction of mixed-metal ternary E−Mn−Cr complexes (E = chalcogen elements) is still a great challenge. Our previously reported trigonal-bipyramidal clusters, $[E_2Mn_3(CO)_9]^-$ (E = S, Se),[14a] were electron-precise anion clusters and could be viewed as potential candidates for incorporation with other nucleophilic or electrophilic transition metal fragments. To extend our studies of the chemistry of mixed Mn−Cr clusters, we have examined the interaction of $[E_2Mn_3(CO)_9]^-$ (E = S, Se) with group 6 chromium carbonyl species, $Cr(CO)_6$, under carefully controlled conditions. This paper describes the full details of the syntheses and characterization of a new family of heterometallic Mn−Cr chalcogenide

Received: April 27, 2011
Published: July 20, 2011

Scheme 1

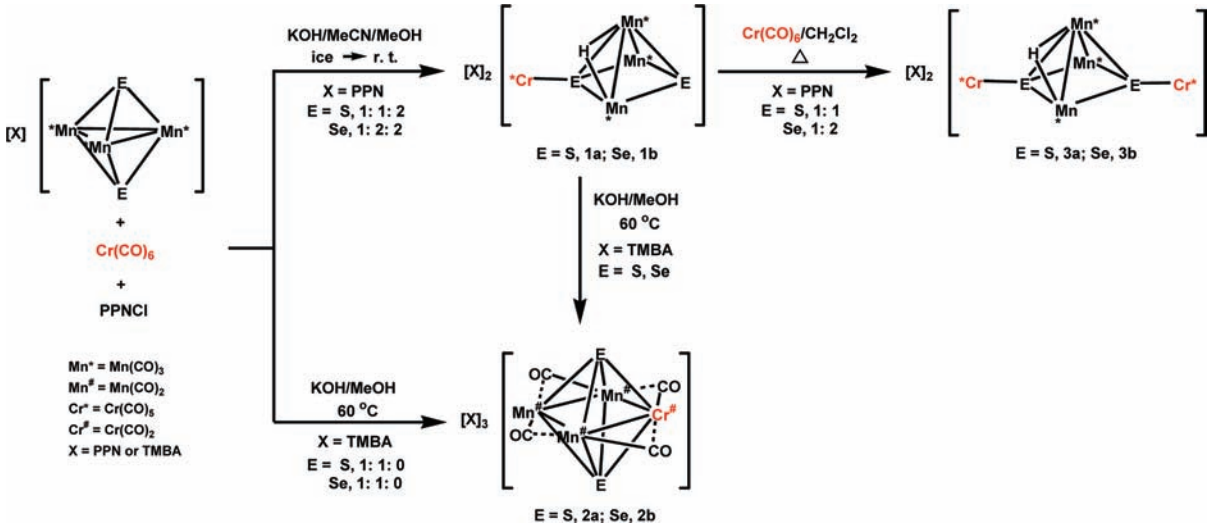

carbonyl cluster complexes, which included three different types of structures, mono- and di-$Cr(CO)_5$-incorporated HE_2Mn_3 square-pyramidal complexes and mono-$Cr(CO)_3$-incorporated E_2Mn_3Cr octahedral complexes. In addition, the electrochemical properties of these mixed Mn−Cr clusters were systematically investigated to address and compare their redox capability in terms of the effect of the incoming chromium group that was either attached to the square-pyramidal E_2Mn_3 core or incorporated into the octahedral E_2M_4 core. Finally, the electronic properties, stepwise cluster-expansion reactions, and electrochemistry of these new Mn−Cr carbonyl sulfides and selenides were further elucidated and discussed on the basis of density functional theory (DFT) calculations.

RESULTS AND DISCUSSION

Synthesis of Complexes $[HE_2Mn_3Cr(CO)_{14}]^{2-}$ (E = S, 1a; Se, 1b). On the basis of the electron-counting rule, trigonal-bipyramidal complexes $[E_2Mn_3(CO)_9]^{-}$[14a] (E = S and Se) are electron-precise species (48 electrons). Although stepwise growth from smaller clusters, $[E_2Mn_3(CO)_9]^-$ (E = S, Se), into larger E-rich or Mn-rich clusters was found, providing facile routes to a series of nanosized manganese carbonyl chalcogenide clusters,[14a,d,e] until now, stepwise, controlled-cluster expansion of $[E_2Mn_3(CO)_9]^-$ (E = S, Se) with other transition metal fragments to form mixed-metal carbonyl chalcogenide clusters had not been explored.

In the present study, when $[PPN][E_2Mn_3(CO)_9]$ was treated with $Cr(CO)_6$ and PPNCl in a molar ratio of 1:1:2 or 1:2:2 in concentrated KOH/MeCN/MeOH solutions (4 M) in an ice−water bath, mono-$Cr(CO)_5$-incorporated HE_2Mn_3-based complexes, $[PPN]_2[HE_2Mn_3Cr(CO)_{14}]$ (E = S, $[PPN]_2$[**1a**]; Se, $[PPN]_2$[**1b**]), were formed in moderate yields of 41 and 44%, respectively (see Scheme 1). Clusters **1a** and **1b** also can be isolated as the $[TMBA]^+$ salts by similar procedures. They were both fully characterized by IR, NMR, ICP-AES, and elemental analysis, as well as single-crystal X-ray diffraction analysis. Oak Ridge thermal ellipsoid plot (ORTEP) diagrams of the structures of **1a** and **1b** were shown in Supporting Information, Figure S1 and Figure 1. Clusters **1a** and **1b** were isostructural species and each displayed an E_2Mn_3 square-pyramidal core (E = S, **1a**; Se, **1b**) with each Mn atom terminally coordinated with three CO's, in which one Mn−Mn bond was bridged by one hydrogen atom and one of the two basal E atoms was externally coordinated with one $Cr(CO)_5$ group.

The ^1H NMR study further confirmed the existence of the hydrides of **1a** and **1b**. For the dianionic **1a**, ^1H NMR gave the hydride resonance at −8.94 ppm. This value is close to the previously reported values for the hydride bridging the Mn−Mn bond in the neutral S_2Mn_2-based species $[Mn_2(CO)_6(\mu\text{-H})\{\mu\text{-}S(SC_3H_5)C{=}C(PPr^i_3)S\}]$[20a] (−7.99 ppm) and $[Mn_2(CO)_6(\mu\text{-H})\{\mu\text{-}S(SR)C{=}C(PCy_3)S\}]$ (R = $SnBu_3$, $SnPh_3$, and $CH_2CH{=}CH_2$)[20b] (−8.59, −8.72, −8.42, respectively). However, it had a greater downfield shift than those in $[Mn_2(CO)_6(\mu\text{-H})(\mu\text{-}S_2CPCy_3)]^-$[20c] (−12.01 ppm) and $[Mn_2(CO)_6(\mu\text{-H})(\mu\text{-}R'SC(S)PR_3)]$[20c] (ranging from −13.43 to −13.77 ppm). On the other hand, the ^1H NMR signal for the hydride of **1b** (−7.78 ppm) was close to that of **1a** (−8.94 ppm). There were no previous examples of hydride-bridged Mn−Mn bonds reported in the Se−Mn system, according to a search of the Cambridge Crystallographic Data Centre.

The formation of the anions **1** was proposed to occur via the $[HCr(CO)_5]^-$[21] attack on the starting clusters $[E_2Mn_3(CO)_9]^-$ (E = S, Se),[14a] followed by the hydride transfer, giving rise to complexes **1a** and **1b**. This hypothesis was supported by the independent experiments that $[E_2Mn_3(CO)_9]^-$ (E = S, Se) readily reacted with the isolated $[HCr(CO)_5]^-$ anion to give clusters **1a** and **1b** with the comparable yields, respectively. In addition, the formation of $[HCr(CO)_5]^-$ anion was detected by IR spectroscopy in the course of the reaction of $[E_2Mn_3(CO)_9]^-$ with $Cr(CO)_6$ in KOH/MeOH/MeCN. Furthermore, the reaction of $[E_2Mn_3(CO)_9]^-$ with reductants such as KOH/MeOH or Na-Ketyl produced the known square-pyramidal clusters $[E_2Mn_3(CO)_9]^{2-}$.[13a,14e] Therefore, the source of the hydride in **1** was most likely from the hydride of $[HCr(CO)_5]^-$ which was produced from the nucleophilic attack of OH^- on CO of $Cr(CO)_6$, followed by the beta-elimination and loss of CO_2.

Synthesis of Octahedral Complexes $[E_2Mn_3Cr(CO)_{12}]^{3-}$ (E = S, 2a; Se, 2b). With careful control of the reaction conditions (the source of the cations and the temperature), the reaction of $[TMBA][E_2Mn_3(CO)_9]$ with $Cr(CO)_6$ in a molar ratio of 1:1 in 4 M KOH/MeOH at 60 °C led to the formation of

dx.doi.org/10.1021/ic200885h |Inorg. Chem. 2011, 50, 7735–7748

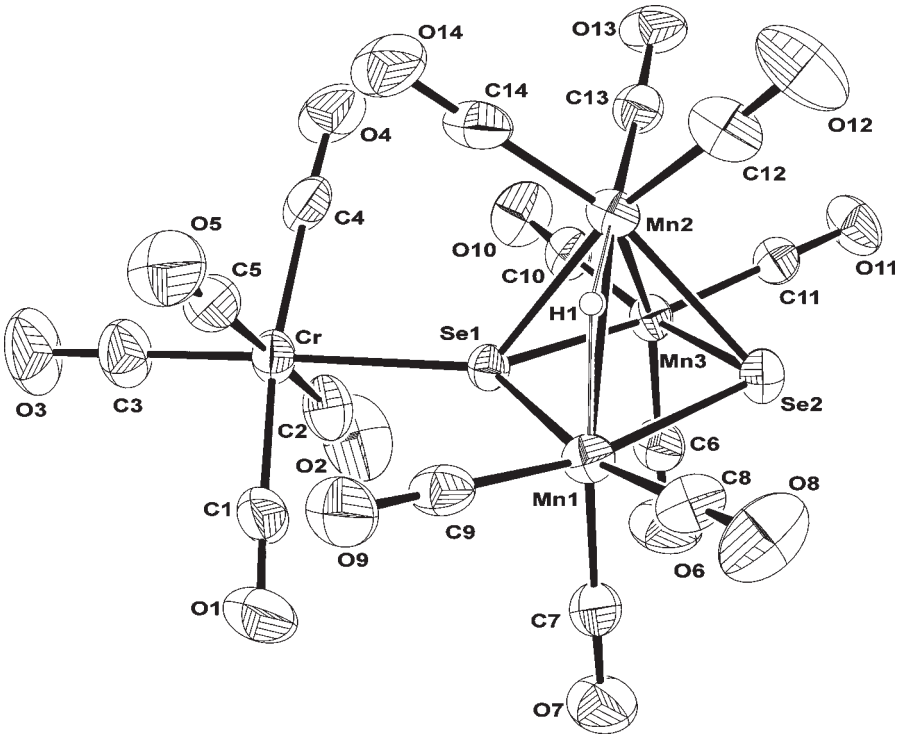

Figure 1. ORTEP diagram (30% thermal ellipsoids) showing the structure and atom labeling for **1b**.

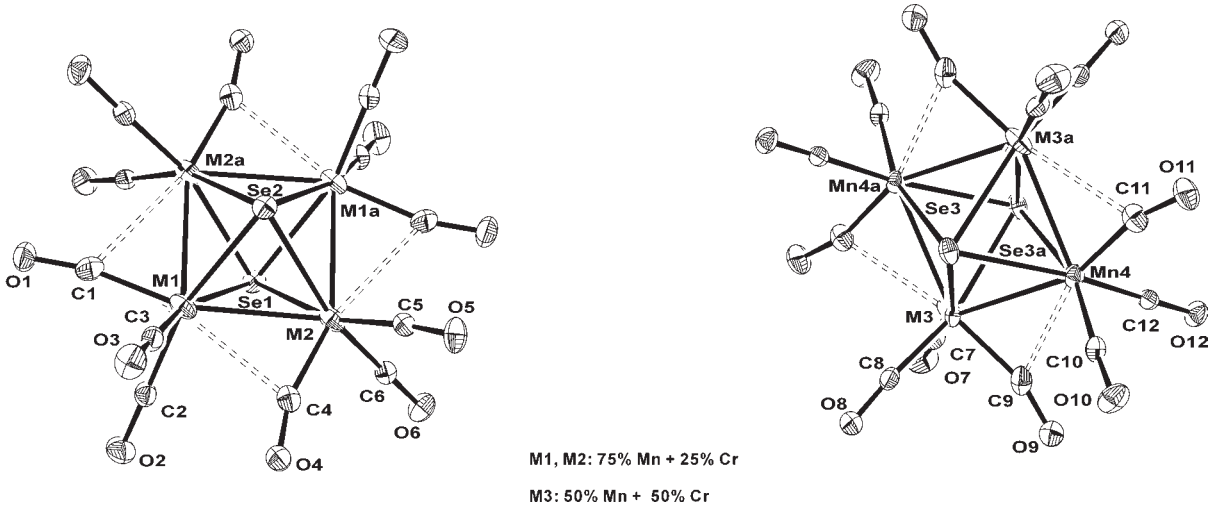

Figure 2. ORTEP diagram (30% thermal ellipsoids) showing the structure and atom labeling for **2b**. CH_2Cl_2 molecules were omitted for clarity.

mono-$Cr(CO)_3$-incorporated octahedral complexes $[TMBA]_3[E_2Mn_3Cr(CO)_{12}]$ (E = S, $[TMBA]_3$[**2a**]; Se, $[TMBA]_3$[**2b**]), respectively (see Scheme 1). The anionic **2a** and **2b** were extremely air- and moisture-sensitive and could only be isolated as the $[TMBA]^+$ salt, but this was not feasible for other cationic salts such as $[PPN]^+$ and $[Et_4N]^+$. The formation of octahedral clusters **2a** and **2b** from trigonal bipyramidal clusters $[E_2Mn_3(CO)_9]^{-}$[14a] (E = S and Se) was complicated by the Mn−Mn bond cleavage, E−Cr and Mn−Cr bond formation, and CO migration from the terminal to the bridging mode. Complexes **2a** and **2b** were also fully characterized using spectroscopic methods. As shown in Supporting Information, Figure S2 and Figure 2, **2a** and **2b** each displayed a bimetallic Mn_3Cr square bicapped above and below by two quadruple-bridging chalcogenide atoms.

Synthesis of Complexes $[HE_2Mn_3Cr_2(CO)_{19}]^{2-}$ (E = S, 3a; Se, 3b). To further investigate the nucleophilicity of the triply bridging μ_3-E ligand of complexes **1a** and **1b**, the reaction of **1a** or **1b** with 1 or 2 equiv of $Cr(CO)_6$ heated in refluxing CH_2Cl_2, respectively, were carried out. These reactions led to the formation of novel cluster-expansion products, di-$Cr(CO)_5$-incorporated HE_2Mn_3-based complexes $[HE_2Mn_3Cr_2(CO)_{19}]^{2-}$ (E = S, **3a**; Se, **3b**), with moderate yields (see Scheme 1). Clusters **3a** and **3b** are isomorphous, and each was shown by X-ray analysis to have two asymmetric $Cr(CO)_5$ groups connected by the square-pyramidal $E_2Mn_3(CO)_9$ core with each Mn atom terminally

dx.doi.org/10.1021/ic200885h |*Inorg. Chem.* 2011, 50, 7735–7748

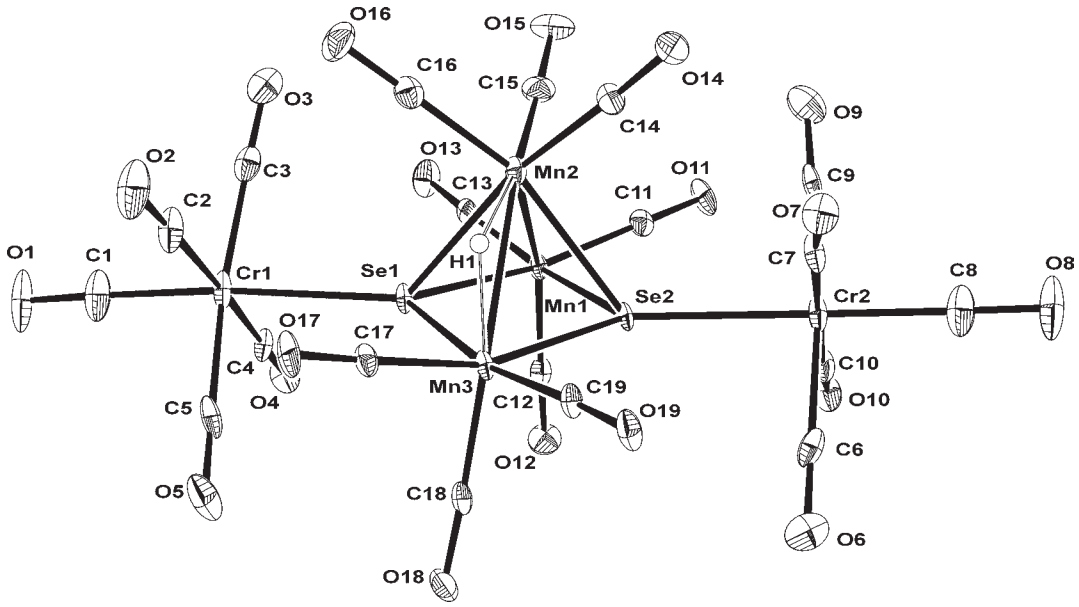

Figure 3. ORTEP diagram (30% thermal ellipsoids) showing the structure and atom labeling for **3b**.

coordinated with three CO's, in which two basal E atoms were both externally coordinated with the $Cr(CO)_5$ groups, with one of the two Mn−Mn bonds bridged by one hydrogen atom (Supporting Information, Figure S3 and Figure 3).

The existence of the hydrides of complexes **3a** and **3b** was confirmed by an ^1H NMR experiment, showing the ^1H NMR singlet at −8.97 and −7.80 ppm, respectively. These values were close to the values of complexes **1a** and **1b** (−8.94, −7.78 ppm), indicative of the minimal effect of an additional $Cr(CO)_5$ fragment. The infrared spectra of **3a** and **3b** showed the absorptions characteristic of terminal carbonyls, with a pattern similar to that of clusters **1a** and **1b**, but with the frequencies shifted to higher energies because of the electron-withdrawing effect of the $Cr(CO)_5$ fragment. This result seems to suggest, as might be expected, that **3a** and **3b** each consisted of an $[H(\mu_3\text{-}E)(\mu_4\text{-}E)Mn_3Cr(CO)_{14}]$ core in which the bare μ_3-E atom was further linked to the introduced $Cr(CO)_5$ unit via the donor−acceptor bond.

Electron Counts of 1a, 1b, 2a, 2b, 3a, and 3b. As shown in Scheme 1, the dianionic clusters **1** (**1a** and **1b**) and **3** (**3a** and **3b**) were all electron-deficient E_2Mn_3-based square-pyramidal complexes with 70 and 86 electrons, respectively. Because the externally bound $Cr(CO)_5$ moiety is thought to donate zero electrons to the metal skeleton, the dianionic clusters **1a**, **1b**, **3a**, and **3b** were found to possess seven skeletal electron pairs each, according to the Wade's rule, in accord with the 7 skeletal electron pairs required for a square pyramidal structure. The octahedral complexes of **2** (**2a** and **2b**) were electron-deficient 66 electron-species, and each possessed a *closo*-geometry with 7 skeletal electron pairs in terms of Wade's rule. The *nido*-clusters **1** and **3** and *closo*-clusters **2** were all found to be diamagnetic species according to SQUID analysis.

Transformation of Complexes 1a and 1b to Octahedral Complexes 2a and 2b. As described above, the reaction of $[E_2Mn_3(CO)_9]^-$ with $Cr(CO)_6$ in 4 M KOH/MeCN/MeOH basic solutions in an ice−water bath produced mono-$Cr(CO)_5$-incorporated HE_2Mn_3-complexes $[HE_2Mn_3Cr(CO)_{14}]^{2-}$ (E = S, **1a**; Se, **1b**), while a similar reaction refluxed at 60 °C led to the formation of mono-$Cr(CO)_3$-incorporated octahedral clusters $[E_2Mn_3Cr(CO)_{12}]^{3-}$ (E = S, **2a**; Se, **2b**). Therefore, clusters **1a** and **1b** were thought to act as the intermediate complexes for the formation of clusters **2a** and **2b**. This was indeed the case. By careful treatment with potassium hydroxide at 60 °C, cluster **1a** or **1b** could be successfully converted into the octahedral cluster **2a** or **2b**, which was accompanied by a remarkable color change from reddish-brown (complexes **1a** and **1b**) to purplish-black (complex **2a**) or greenish-black (complex **2b**). Simultaneously, the ^1H NMR spectra showed that the hydride signals of **1a** and **1b** disappeared as they transformed into complexes **2a** and **2b**. In addition, the CO frequencies for *closo*-**2a** and **2b** were quite similar, but shifted to low energies compared to those for *nido*-**1a** and **1b**, because of the pronounced effect of the charge. In a previous study, it was postulated that the square pyramidal complex with a pendant metal fragment could be the key intermediate for the formation of an octahedral complex.[22] However, there were no experimental examples to directly verify this assumption. The present study demonstrated a novel example of a facile conversion from a metal fragment-attached square pyramidal structure to the octahedral geometry. Moreover, the metal-core closure of clusters **1a** and **1b** to give octahedral clusters **2a** and **2b** upon treatment with KOH will be discussed later with the theoretical calculations.

X-ray Structural Comparison of $[Et_4N]_2$[1a], $[PPh_4]_2$[1b], [TMBA]$_3$[2a]·CH_2Cl_2, [TMBA]$_3$[2b]·$0.5CH_2Cl_2$, $[PPN]_2$[3a], and $[PPN]_2$[3b]. As shown in Supporting Information, Figure S1 and Figure 1, complexes **1a** and **1b** each displayed a square-pyramidal E_2Mn_3 core with one E atom bonded to an additional $Cr(CO)_5$ fragment, in which each cluster contained a nearly planar E_2Mn_2 base, with average distances of 0.090 and 0.073 Å, respectively, to the least-squares plane. The three Mn atoms of clusters **1a** and **1b** were six-, seven-, and eight-coordinated, respectively. The hydride of **1a** or **1b** across one Mn−Mn bond was refined with an isotropic temperature factor, in which the H−Mn distances in **1a** or **1b** were not equal (1.5929(9)/1.8362(8) Å, **1a**; 1.69(4)/1.66(4) Å, **1b**).

Clusters **1a** and **1b** possessed four metal atoms: one chromium and three manganese. These four metal atoms were assembled in

Table 1. Averaged Bond Distance (Å) for $[PPN]_2[1a]$, $[PPh_4]_2[1b]$, $[TMBA]_3[2a]\cdot CH_2Cl_2$, $[TMBA]_3[2b]\cdot 0.5CH_2Cl_2$, $[PPN]_2[3a]$, $[PPN]_2[3b]$, and Related Complexes

complex	E−Mn	Mn−Mn	E−Cr	H−Mn	Mn−Cr	ref
$[PPN]_2[\mathbf{1a}]$	2.32(2)	2.69(2)	2.427(2)	1.7(2)		*a*
$[PPh_4]_2[\mathbf{1b}]$	2.43(3)	2.78(2)	2.532(1)	1.68(2)		*a*
$[TMBA]_3[\mathbf{2a}]\cdot CH_2Cl_2$	2.40(2)	2.68(4)	2.35(6)		2.6(3)	*a*
$[TMBA]_3[\mathbf{2b}]\cdot 0.5CH_2Cl_2$	2.51(1)	2.73(4)	2.49(5)		2.73(3)	*a*
$[PPN]_2[\mathbf{3a}]$	2.32(2)	2.72(2)	2.45(1)	1.6(2)		*a*
$[PPN]_2[\mathbf{3b}]$	2.43(2)	2.76(1)	2.533(4)	1.7(1)		*a*
$[PPN][S_2Mn_3(CO)_9]$	2.24(1)	2.768(3)				12g
$[Et_4N][Se_2Mn_3(CO)_9]$	2.36(2)	2.83(2)				14a
$[PPh_4]_2[Se_2Mn_3(CO)_9]$	2.43(2)	2.76(6)				13a
$[PPN]_2[Se_2Mn_4(CO)_{12}]$	2.475(2)	2.705(8)				14a
$[Cp_2Cr_2(\mu\text{-}SCMe_3)(\mu_3\text{-}S)_2Mn(CO)_3]$	2.29(2)		2.30(4)		2.77(8)	18b
$[CrMn_2(CO)_8(\mu\text{-}CO)_2(\mu_3\text{-}SN_2C_4H_5)_2]$	2.320(2)		2.343(2)		2.849(1)	25
$[CpMnSe_2Cr(CO)_7]$	2.50(1)		2.503(2)			19a
$[CpMnSe_2Cr_2(CO)_{12}]$	2.53(2)		2.50(1)			19a
$[Et_4N]_2[Se_2Mn_3(CO)_{10}\{Cr(CO)_5\}_2]$	2.43(2)	2.671(2)	2.541(1)			19c

[a] This work.

a cluster bridged by the chalcogen atoms with two different bonding modes: E(2) is a triply bridging atom that bridges three manganese atoms, but E(1) is a quadruple-bridging atom that bridges three manganese atoms and a pendant $Cr(CO)_5$ group. To the best of our knowledge, the related mixed-metal carbonyl chalcogenide clusters containing both μ_3- and μ_4-E bonding modes are limited to the neutral complexes: $[CpRe_2Mo(CO)_8(\mu_3\text{-}S)(\mu_4\text{-}S)CpMo(CO)_3]$,[23a] $[Fe_2Mn(CO)_9(\mu_3\text{-}S)(\mu_4\text{-}S)Mn(CO)_5]$,[23b] $[CpMoMn_2(CO)_9(\mu_3\text{-}S)(\mu_4\text{-}S)Mn(CO)_4]$,[23c] $[Os_3(CO)_9(\mu_3\text{-}S)(\mu_4\text{-}S)W(CO)_5]$,[23d] $[Fe_3(CO)_9(\mu_3\text{-}S)(\mu_4\text{-}S)W(CO)_4PMe_2Ph]$,[23e] $[\{P(CH_2Ph)Ph_2\}_2Ru_3(CO)_7(\mu_3\text{-}Se)(\mu_4\text{-}Se)W(CO)_5]$,[22] and $[Co_3(CO)_7(\mu_3\text{-}Te)(\mu_4\text{-}Te)Nb(C_5Me_4Et)_2]$,[23f] and no examples of anionic mixed-metal carbonyl chalcogenides were ever reported prior to the present study. A search of the Cambridge Crystallographic Data failed to identify any structurally characterized E−Mn−Cr compound that contained both μ_3- and μ_4-E bonding modes. Clusters **1a** and **1b** represent the first examples of E−Mn−Cr clusters possessing both μ_3- and μ_4-E bonding modes.

Clusters **2a** and **2b** were isostructural, and each contained two structurally independent entities in the unit cell. As shown in Supporting Information, Figure S2 and Figure 2, clusters **2a** and **2b** each had a crystallographic center of symmetry at the center of the disordered E_2M_4 octahedral core (E = S, **2a**; Se, **2b**). The square heterometallic M_4 unit in **2a** or **2b** was supported by two Mn−Mn and two Mn−Cr bonds, with two μ_4-E atoms capping above and below the M_4 plane. In **2a**, each M atom of the M_4 square in the two independent forms was coordinated with two terminal CO's and one semibridging CO, where Mn(1), Mn(2), Mn(3), and Mn(4) atoms and Cr(1), Cr(2), Cr(3), and Cr(4) atoms of the squares were disordered with 75 and 25% occupancy, respectively. In **2b**, one independent square M_4 plane showed the disordered M(1) and M(2) atoms where Mn and Cr are with 75 and 25% occupancy, and the other one showed the disordered M(3) atom with Mn and Cr present in a 50:50 ratio. According to a literature search, clusters **2a** and **2b** were structurally similar to the other neutral mixed-metal E_2M_4 octahedral complexes: $[(\mu_4\text{-}S)_2Ru_3W(CO)_{11}(PMe_2Ph)]$,[24a] $[(\mu_4\text{-}Se)_2Fe_3Ru(CO)_{10}(\mu\text{-}CO)]$,[24b] $[(\mu_4\text{-}Se)_2WRu_3(\mu\text{-}CO)_4(CO)_6(L)_2]$ (L = phosphane),[22] $[(\mu_4\text{-}S)_2PtRu_3(CO)_6(\mu\text{-}CO)_2(\eta^2\text{-}P{-}P)]$ (P−P = dppf or dppr),[24c] and $[(\mu_4\text{-}Se)_2WRu_3(\mu\text{-}CO)_4(CO)_7(L)]$ (L = phosphine ligand).[24d] Clusters **2a** and **2b** represent the first examples of mixed group 7 and 6 carbonyl chalcogenide complexes in this octahedral E_2M_4 arrangement.

As shown in Supporting Information, Figure S3 and Figure 3, clusters **3a** and **3b** were isomorphous, and each contained five metal atoms: two chromium and three manganese. These five metal atoms are assembled in a cluster that is bridged by two quadruple μ_4-E atoms (E = S, **3a**; Se, **3b**) with one hydride across one Mn−Mn bond. They could also be regarded as di-$Cr(CO)_5$ groups sandwiching a HE_2Mn_3 metal core, or the μ_3-E atom of complexes **1a** and **1b** further bonded to a secondary $Cr(CO)_5$ group. X-ray analysis of complex **3a** revealed that C(3), O(3); C(4), O(4); C(5), O(5); and C(17), O(17) atoms in the four terminal CO's of the di-$Cr(CO)_5$ fragments were disordered with 50, 55, 55, and 60% occupancy, respectively (see Supporting Information, Figure S3). Similar to **1a** and **1b**, complexes **3a** and **3b** each contained a very slightly distorted E_2Mn_2 base of the E_2Mn_3 metal core, with average distances of 0.082 and 0.040 Å, respectively, to the least-squares planes, regardless of the effect of the two attached $Cr(CO)_5$ groups. This novel type of structural feature containing both the H-bridged Mn−Mn bond and the two μ_4-E quadruple-bridging atoms is the only example reported in main group-containing manganese complexes.

For further comparison, the distances of the E−Mn, Mn−Mn, E−Cr, H−Mn, and Mn−Cr bonds of $[PPN]_2[\mathbf{1a}]$, $[PPh_4]_2[\mathbf{1b}]$, $[TMBA]_3[\mathbf{2a}]\cdot CH_2Cl_2$, $[TMBA]_3[\mathbf{2b}]\cdot 0.5CH_2Cl_2$, $[PPN]_2[\mathbf{3a}]$, $[PPN]_2[\mathbf{3b}]$, and related complexes are listed in Table 1. In general, the corresponding E−Mn, Mn−Mn, and E−Cr averaged bond distances in these new E−Mn−Cr clusters were similar to those reported for related complexes.[12g,13a,14a,18b,19a,19c,25] The average Mn−Cr distances in **2a** and **2b** were 2.6(3) and 2.73(3) Å, which are comparatively shorter than those found in $[Cp_2Cr_2(\mu\text{-}SCMe_3)(\mu_3\text{-}S)_2Mn(CO)_3]$ (2.77(8) Å)[18b] and $[CrMn_2(CO)_8(\mu\text{-}CO)_2(\mu_3\text{-}SN_2C_4H_5)_2]$ (2.849(1) Å),[25] suggesting stronger Mn−Cr bonding because of the *closo*-octahedral skeleton. The corresponding average E−Mn, Mn−Mn, E−Cr, and H−Mn distances of **1a**, **1b**, **3a**, and **3b** were similar, because of the small effect of the secondary $Cr(CO)_5$ group. In addition,

dx.doi.org/10.1021/ic200885h |*Inorg. Chem.* 2011, 50, 7735–7748

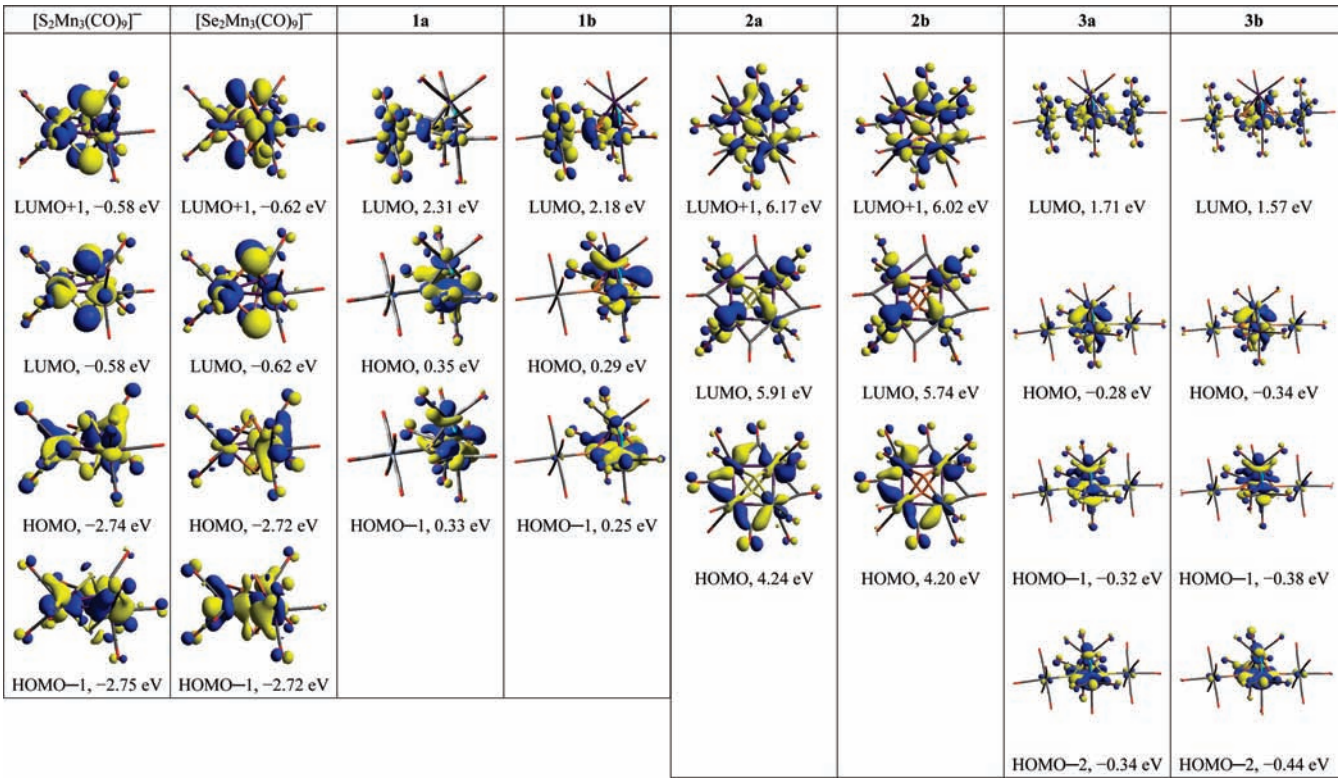

Figure 4. Spatial graphs (isovalue = 0.04) of the selected frontier molecular orbitals and their associated calculated energies of $[S_2Mn_3(CO)_9]^-$, $[Se_2Mn_3(CO)_9]^-$, **1a**, **1b**, **2a**, **2b**, **3a**, and **3b**.

the Mn−Mn and E−Cr bond lengths of **2a** and **2b** were slightly shorter than those of **1a** and **1b**, while the E−Mn bond lengths of **2a** and **2b** were longer than those of **1a** and **1b**, probably because of the increased bonding character associated with the Cr atom. Moreover, in general, the distances of E−Mn, Mn−Mn, E−Cr, H−Mn, and Mn−Cr in the Se_2-based Mn−Cr complexes were slightly longer than the S_2-based Mn−Cr complexes because of the larger atomic radius of the Se atom compared with the S atom. It is also interesting to note that the size of $[E_2Mn_3(CO)_9]^-$ (E = S, Se), **1**, **2**, and **3** including CO's were approximately 0.774(0.884), 0.976(1.004), 0.895(0.898), and 1.366(1.404) nm, respectively, indicative of controllable stepwise construction of these nanosized clusters.

DFT Calculations. The DFT method was employed to further describe the electronic structures of $[E_2Mn_3(CO)_9]^-$ (E = S, Se) and **1**−**3** to rationalize their relevant reactions. All the calculations were carried out at the BP86[26,27] and B3LYP[28,29] functional levels (Supporting Information, Table S1). The TZVP[30] basis set was applied for all atoms in each complex for these calculations. The geometries of $[E_2Mn_3(CO)_9]^-$ (E = S, Se) and **1**−**3** were also fully optimized with the same level of theory. Basically similar results were obtained with the BP86 and B3LYP functionals. However, the former provided a better correlation with experimental parameters (Supporting Information, Table S2) and was used for analysis of the frontier orbitals. The level of BP86 may be more reliable and work better than B3LYP for many organometallic systems.[31−33] Therefore, the present study was focused on the analysis of the geometrical results provided by BP86/TZVP calculations. In addition, the Wiberg bond indices[34] and natural population analyses (NPA)[35] for these complexes were calculated, and the results are listed in Supporting Information, Table S3.

Formation of Clusters 1 and 3. The DFT calculations showed that the active sites of $[E_2Mn_3(CO)_9]^-$ (E = S, Se) for the formation of clusters **1** (**1a** and **1b**) could be related to the lowest unoccupied molecular orbitals (LUMO) and LUMO+1 of $[E_2Mn_3(CO)_9]^-$. As shown in Figure 4 and Table 2, the LUMO and LUMO+1 of the respective $[E_2Mn_3(CO)_9]^-$ (E = S, Se) were degenerate, and each had major contributions from the p orbital of the E atoms and d and p orbitals of the Mn atoms. It is reasonable to propose that the incoming chromium anions "$[HCr(CO)_5]^-$/$[Cr(CO)_5]^{2-}$"[21] could interact with the "E" site of $[E_2Mn_3(CO)_9]^-$, presumably accompanied by the hydrogen atom bridging two Mn atoms, to form new E−Cr and H−Mn bonds accompanied by one Mn−Mn bond breakage, to give rise to complexes **1a** and **1b**. Hence, the formation of complexes **1a** and **1b** was not only dominated by the frontier orbitals, but also was induced by the Mn−Mn bond breakage of $[E_2Mn_3(CO)_9]^-$ (E = S, Se), which reflected on their weaker Wiberg bond indices (0.279 and 0.285). As shown in Figure 4, the highest occupied molecular orbitals (HOMO) of **1a** and **1b** received major contributions from the p orbital of the E atoms (**1a**/**1b**, μ_3-E, 10.24/19.01%; μ_4-E, 4.04/0.14%) and d orbital of the Mn atoms (**1a**/**1b**, 62.41/59.94%). This suggests that the "μ_3-E" atoms of **1a** and **1b** were reactive sites for the secondary chromium fragment $Cr(CO)_5$ to form **3a** and **3b**, respectively, which was also supported by their space-filling models (see Figure 5).

Proposed Pathway from 1a(1b) to 2a(2b). The formation of cluster **2a**(**2b**) is likely to occur via a nucleophilic attack of OH^- on CO of the pendant $Cr(CO)_5$ fragment of complex **1a**(**1b**), followed by loss of CO_2, forming a "$HCr(CO)_4$" fragment, followed by the Mn−Cr and E−Cr bond formation accompanied with H_2 reductive elimination. This proposed pathway was

dx.doi.org/10.1021/ic200885h |*Inorg. Chem.* 2011, 50, 7735–7748

Table 2. Calculated Components of the Selected Frontier Molecular Orbitals for $[E_2Mn_3(CO)_9]^-$ (E = S, Se), 1a, 1b, 2a, 2b, 3a, 3b

	atoms						
complex	E	Mn	Cr	H	CO	$HE_2Mn_3(CO)_9$ /$E_2Mn_3(CO)_9$ (sum)	$Cr_m(CO)_n$ (sum)
				$[E_2Mn_3(CO)_9]^-$ (E = S)			
LUMO+1	23.78	50.61			25.61	100	0
LUMO	23.79	50.62			25.59	100	0
HOMO	5.92	68.28			25.80	100	0
HOMO−1	6.90	65.90			27.20	100	0
				$[E_2Mn_3(CO)_9]^-$ (E = Se)			
LUMO+1	26.60	49.90			23.50	100	0
LUMO	26.71	49.87			23.52	100	0
HOMO	7.97	67.10			24.93	100	0
HOMO−1	7.96	67.08			24.96	100	0
				1a			
LUMO (m = 1, *n* = 5)	3.44	20.67	16.13	0.06	59.70	40.69	59.31
HOMO (m = 1, *n* = 5)	14.28	62.41	0.69	0.30	22.32	98.86	1.14
				1b			
LUMO (m = 1, *n* = 5)	3.76	26.11	15.04	0.01	55.08	48.35	51.65
HOMO (m = 1, *n* = 5)	19.15	59.94	0.06	0.06	20.79	99.92	0.08
				2a			
LUMO (m = 1, *n* = 3)	3.26	53.87	8.00		34.87	86.53	13.47
HOMO (m = 1, *n* = 3)	0.49	51.86	14.01		33.64	80.55	19.45
				2b			
LUMO (m = 1, *n* = 3)	3.91	52.46	8.76		34.87	85.54	14.46
HOMO (m = 1, *n* = 3)	0.32	55.17	10.72		33.79	85.44	14.56
				3a			
LUMO (m = 2, *n* = 10)	2.90	31.45	12.04	0.02	53.59	55.98	44.02
HOMO (m = 2, *n* = 10)	12.66	53.16	8.20	0.01	25.97	86.44	13.56
				3b			
LUMO (m = 2, *n* = 10)	3.18	36.91	10.62	0.02	49.27	63.58	36.42
HOMO (m = 2, *n* = 10)	15.57	51.58	8.60	0.01	24.24	86.28	13.72

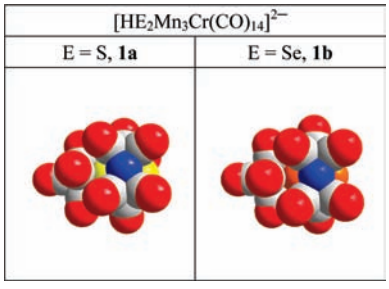

Figure 5. Space filling structures of **1a** and **1b** (yellow: S atoms; Orange: Se atoms; blue: H atom; red: O atoms; white: C atoms).

supported by that the LUMO orbital of **1a** or **1b** was mainly contributed from the $Cr(CO)_5$ fragment (59.31%, **1a**; 51.65% **1b**). Furthermore, the relative Gibb's free energies ΔG(298 K), calculated by BP86 in MeOH, for the transformation of **1a** or **1b** into **2a** or **2b** ($[HE_2Mn_3Cr(CO)_{14}]^{2-}$ (E = S, **1a**; Se, **1b**) + OH^- → $[E_2Mn_3Cr(CO)_{12}]^{3-}$ (E = S, **2a**; Se, **2b**) + CO_2 + H_2+ CO) were thermally favorable (ΔG: −27.47 kcal/mol, E = S; ΔG: −24.30 kcal/mol, E = Se).

Electrochemistry. In view of the effect of the $Cr(CO)_x$ fragment on the E_2Mn_3 (E = S, Se) core and structural relationships among complexes **1a**, **1b**, **2a**, **2b**, **3a**, and **3b**, their electrochemical properties were investigated using cyclic voltammetry (CV) and differential pulse voltammetry (DPV) in MeCN under N_2, which was further compared with the related trigonal-pyramidal clusters $[E_2Mn_3(CO)_9]^-$ (E = S, Se[14e]). The CVs of these clusters were somewhat broad and could not be assigned unambiguously. Therefore, DPV studies were carried out to explore the redox behavior of these clusters. The electrochemical data for each complex studied are listed in Table 3 and Supporting Information, Table S4, and the DPVs and CVs are shown in Figure 6 and Supporting Information, Figures S4 and S5, respectively. The scan range was set between ∼ +1.00 to ∼ −1.00 V, because of the interference of $[PPN]^+$ and $[TMBA]^+$.

For the DPV measurements, the electron stoichiometry is determined by the measurement of the peak width at half-height ($W_{1/2}$).[36] As seen in Figure 6 and Supporting Information, Figure S4, the widths of the DPV peaks at half-height of $[PPN][E_2Mn_3(CO)_9]$ (E = S, Se) and clusters **1**−**3** (Table 3) were a bit greater than the value ($W_{1/2}$ = 90 mV) expected for

dx.doi.org/10.1021/ic200885h |*Inorg. Chem.* 2011, 50, 7735–7748

Table 3. Differential Pulse Voltammetry of [PPN][$S_2Mn_3(CO)_9$], [PPN][$Se_2Mn_3(CO)_9$], [PPN]$_2$[1a], [PPN]$_2$[1b], [TMBA]$_3$[2a], [TMBA]$_3$[2b], [PPN]$_2$[3a], [PPN]$_2$[3b], and $Cr(CO)_6$

	oxidation process		reduction process	
complex	Ep^{ox}/V[a] ($W_{1/2}$/mV[c])	Ep^{red}/V[b] ($W_{1/2}$/mV[c])	Ep^{ox}/V[a] ($W_{1/2}$/mV[c])	Ep^{red}/V[b] ($W_{1/2}$/mV[c])
[PPN][$S_2Mn_3(CO)_9$]	0.605 (130)	0.645 (130)		
[PPN][$Se_2Mn_3(CO)_9$][e]	0.554 (110)	0.601 (118)		
[PPN]$_2$[**1a**]	0.756 (90)	0.796 (101)		
	0.604 (130)	0.656 (135)		
	0.328 (90)	0.396 (93)		
	0.032 (130)	0.060 (150)		
[PPN]$_2$[**1b**]	0.883 (142)	0.877 (111)		
	0.551 (105)	0.561 (115)		
	0.359 (100)	0.337 (99)		
	0.127 (100)	0.121 (115)		
[TMBA]$_3$[**2a**]	0.702 (138)	0.666 (132)	−0.046 (106)	−0.050 (100)
	0.542 (130)		−0.270 (111)	−0.258 (115)
	~0.350 ([d]) (br)	0.366 (98)	−0.690 (115)	−0.702 (108)
[TMBA]$_3$[**2b**]	0.702 (138)		−0.050 (110)	−0.044 (104)
	0.538 (136)	0.544 (96)	−0.274 (112)	−0.234 (101)
	~0.370 ([d]) (br)	0.368 (100)	−0.694 (115)	−0.684 (108)
[PPN]$_2$[**3a**]	0.867 (128)	0.872 (129)	−0.137 (210) (br)	−0.160 (212) (br)
	0.755 (99)	([d]) (br)		
	0.675 (95)	~0.688 ([d]) (br)		
	0.595 (91)	([d]) (br)		
	0.323 (92)	0.324 (110)		
[PPN]$_2$[**3b**]	0.849 (133)	0.853 (105)		−0.182 (150) (br)
	0.693 (115)	([d]) (br)		
	0.561 (173)	([d]) (br)		
	0.325 (80)	0.345 (84)		
	0.069 (91)			
$Cr(CO)_6$			−0.063 (493) (br)	−0.233 (415) (br)

[a] Ep^{ox} = oxidative peak potential. [b] Ep^{red} = reductive peak potential. [c] $W_{1/2}$ = width at half-height. [d] Difficult to determine. [e] ref 14e.

one-electron reversible redox reactions, indicating that these DPV responses were quasi-reversible.[37] As listed in Table 3, mono-$Cr(CO)_5$-incorporated **1a** an **1b** each had four one-electron quasi-reversible oxidations, at +0.032 to +0.756 V and +0.127 to +0.883 V, respectively. The DFT calculations showed that the HOMO and HOMO−1 of **1a** and **1b** were mainly localized on the E_2Mn_3 moieties, suggesting that the oxidation processes of **1a** and **1b**, mainly occurred in the E_2Mn_3 core (Table 2 and Figure 4), indicative of a small effect of the attached mono-$Cr(CO)_5$ fragment. The rich quasi-reversible oxidation processes observed for the E_2Mn_3Cr-based complexes, **1a** and **1b**, were ascribed to the positive energy levels of the almost degenerate HOMO and HOMO−1 orbitals in each cluster (Figure 4). However, octahedral complexes, **2a** and **2b**, each exhibited two one-electron quasi-reversible oxidations at approximately +0.350 to +0.702 V and +0.370 to +0.538 V and three one-electron quasi-reversible reductions at −0.050 to −0.702 V and −0.044 to −0.684 V, respectively. The oxidative and reductive waves for **2a** and **2b** were tentatively assigned as the oxidations and reductions occurred in the square heterometallic M_4 units, according to the HOMO and LUMO as well as LUMO+1 levels (Figure 4). In addition, the calculated components of Mn_3Cr in the LUMO for **2a** and **2b** (61.87 and 61.22%) were significantly greater than those for **1a** and **1b** (36.80 and 41.15%) (Table 2), supportive of the ease and richness of the quasi-reversible reductions of **2a** and **2b**, implying their potential use as electron sponges.[5b,8]

On the other hand, the DPV of the di-$Cr(CO)_5$-incorporatd complex **3a** revealed five one-electron quasi-reversible redox oxidations at +0.323 to +0.867 V and one quasi-reversible redox reduction at −0.160 V, whereas **3b** displayed five one-electron quasi-reversible redox oxidations at +0.325 to +0.849 V (see Figure 6 and Supporting Information, Figure S4). The rich quasi-reversible oxidations of **3a** and **3b** may be related to their narrow-spaced HOMO, HOMO−1, and HOMO−2 orbitals (Figure 4). Besides, these frontier orbitals for **3a** and **3b** mainly arose from the E_2Mn_3 metal core and di-$Cr(CO)_5$ fragment, indicating that the oxidation and reduction processes both occurred mainly in the E_2Mn_3 metal core and the di-$Cr(CO)_5$ fragments (Figure 4). In general, these quasi-reversible oxidation waves for complex **3a** occurred at more positive potentials than those for complex **1a**, which indicated that **3a** was difficult to oxidize because of the two electron-withdrawing $Cr(CO)_5$ fragments (Figure 6). In particular, the first quasi-reversible oxidation wave of **3a** (+0.323 V) displayed a pronounced anodic shift (291 mV) compared to that of **1a** (+0.032 V), which was supported by the calculations that cluster **3a** showed a lower HOMO energy level, decreasing components of HOMO, and decreased nature charges of the $HS_2Mn_3(CO)_9$ core, as well as greater ionization energy,

dx.doi.org/10.1021/ic200885h |Inorg. Chem. 2011, 50, 7735–7748

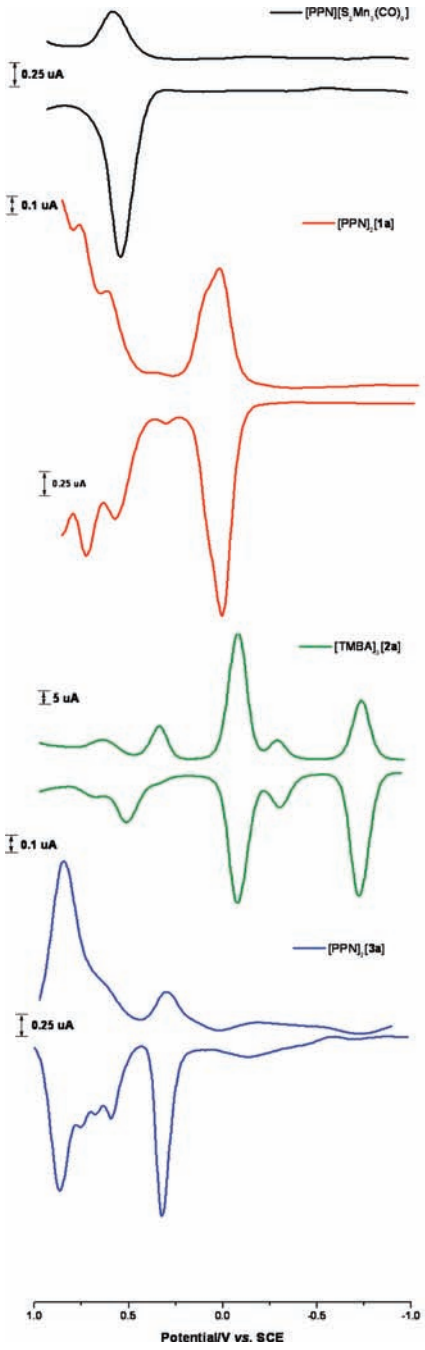

Figure 6. DPVs in MeCN for $[PPN][S_2Mn_3(CO)_9]$ (black), $[PPN]_2$[**1a**] (red), $[TMBA]_3$[**2a**] (green), and $[PPN]_2$[**3a**] (blue). Conditions: electrolyte, 0.1 M Bu_4NClO_4; working electrode, platinum; scan rate, 100 mV s^{-1}. Potentials are vs SCE.

compared with those calculated for **1a** (**3a** vs **1a**: −0.28 vs 0.35 eV; 86.44 vs 98.86%; −0.865 vs −1.383 |e|; IE ≈ $E_{elec}(N-1) - E_{elec}(N)$, 36.59 vs 19.93 kcal/mol, respectively).

CONCLUSIONS

The present study demonstrated that the chalcogen elements of the E_2Mn_3 metal core (E = S, Se) played an important role in the controlled stepwise construction of a new series of mono- or di-$Cr(CO)_5$-incorporated HE_2Mn_3-based complexes **1** and **3**, and mono-$Cr(CO)_3$-incorporated E_2M_4-based octahedral complexes **2**, under different reaction conditions, and the subsequent transformation of **1** (**1a** and **1b**) into octahedral complexes of **2** (**2a** and **2b**) was also achieved. In addition, the electrochemical properties of these resultant E−Mn−Cr complexes displayed quasi-reversible redox waves over quite a large window (+0.883 ∼ −0.702 V). These results can be summarized by the following conclusions. First, the unexpected electron-sponge behavior was observed for complexes **1a** and **1b** and octahedral complexes **2a** and **2b**, which can be readily fine-tuned by the control of electronic properties exhibited by the attached mono-$Cr(CO)_x$ fragment in different metal cores (HE_2Mn_3 vs E_2M_4). Second, in the cases of **1a** and **3a**, significant anodic shifts were observed as a higher number of $Cr(CO)_5$ groups incorporated into the HS_2Mn_3 metal core, because of the pronounced electron-withdrawing ability of the di-$Cr(CO)_5$ groups. Furthermore, the stepwise cluster-growth processes, metal skeleton transformations, electronic properties, and electrochemistry of these E−Mn−Cr carbonyl clusters were rationalized by molecular orbital calculations at the BP86 level of the DFT.

EXPERIMENTAL SECTION

All reactions were performed under an atmosphere of pure nitrogen using standard Schlenk techniques.[38] Solvents were purified, dried, and distilled under nitrogen prior to use. KOH (J. T. Baker), $Cr(CO)_6$ (Strem), PPNCl (Strem), and TMBACl (ACROS) were used as received. $[PPN][E_2Mn_3(CO)_9]$, $[TMBA][E_2Mn_3(CO)_9]$ (E = S, Se), and $[PPN][HCr(CO)_5]$ were prepared according to published methods.[14a,21e] The ^{1}H NMR spectra were taken on a Bruker AV 400 at 400.13 MHz. ^{1}H chemical shifts are reported in ppm and were referenced internally with respect to the solvent resonances (^{1}H, δ = 2.49 for DMSO-d_5). Infrared spectra were recorded on a Perkin-Elmer Paragon 500 IR spectrometer as solutions in CaF_2 cells. Elemental analyses of C, H, and N were performed on a Perkin-Elmer 2400 analyzer at the NSC Regional Instrumental Center at National Taiwan University, Taipei, Taiwan. The manganese and chromium contents of complexes **1**, **2**, and **3** were determined with an inductively coupled plasma-atomic emission (ICP-AES) spectrometer (Perkin-Elmer Optima 3000DV) at the NSC Regional Instrumental Center at National Tsing Hua University, Hsinchu, Taiwan.

Synthesis of $[PPN]_2[HS_2Mn_3Cr(CO)_{14}]$ ($[PPN]_2$[1a]). *Method A.* MeOH (10 mL)/MeCN (5 mL) was added to a mixture of $[PPN][S_2Mn_3(CO)_9]$ (0.66 g, 0.65 mmol), $Cr(CO)_6$ (0.14 g, 0.64 mmol), PPNCl (0.76 g, 1.32 mmol), and KOH (3.39 g, 60.4 mmol) in an ice−water bath. The mixture was stirred at room temperature for 3 h. The solid was collected by filtration, washed with deionized water and MeOH, and then extracted with CH_2Cl_2, which was recrystallized with CH_2Cl_2/MeOH/Et_2O to give a reddish-brown sample of $[PPN]_2[HS_2Mn_3Cr(CO)_{14}]$ ($[PPN]_2$[**1a**]) (0.45 g, 0.26 mmol) (yield: 41% based on $Cr(CO)_6$). IR (ν_{CO}, CH_2Cl_2): 2054 (w), 1967 (vs), 1963 (vs), 1928 (w), 1894 (m), 1869 (m) cm^{-1}. ^{1}H NMR (400 MHz, DMSO-d_6, 300 K): δ −8.94 (s, hydride) (Chemical shifts not given for $[PPN]^+$). Anal. Calcd for $[PPN]_2$[**1a**]: C, 58.98; H, 3.51; N, 1.60. Found: C, 59.14; H, 3.52; N, 1.47. Crystals of $[PPN]_2$[**1a**] suitable for X-ray diffraction were grown from CH_2Cl_2/MeOH/Et_2O. ICP-AES: Mn:Cr = 3.18:1.

Similar procedures were applied for the preparation of $[TMBA]_2[HS_2Mn_3Cr(CO)_{14}]$ by using $[TMBA][S_2Mn_3(CO)_9]$ (0.92 g, 1.46 mmol), $Cr(CO)_6$ (0.33 g, 1.50 mmol), TMBACl (0.84 g, 4.57 mmol), and KOH (4.55 g, 81 mmol) in MeOH (15 mL)/MeCN (5 mL). The yield was 1.06 g (1.09 mmol) of ($[TMBA]_2$[**1a**]) (75% based on $[TMBA][S_2Mn_3(CO)_9]$.)

Method B. MeOH (15 mL)/MeCN (5 mL) was added to a mixture of $[PPN][S_2Mn_3(CO)_9]$ (0.38 g, 0.37 mmol) and $[PPN][HCr(CO)_5]$ (0.28 g, 0.38 mmol) in an ice−water bath. The mixture was stirred at

dx.doi.org/10.1021/ic200885h |*Inorg. Chem.* 2011, 50, 7735–7748

room temperature for 3 h. A methanol solution of PPNCl (0.49 g, 0.85 mmol) was added dropwise into the resulting solution, precipitating the solid. The solid was worked up as mentioned above to give a reddish-brown sample of $[PPN]_2$[**1a**] (0.38 g, 0.22 mmol) (yield: 59% based on $[PPN][S_2Mn_3(CO)_9]$).

Synthesis of $[PPN]_2[HSe_2Mn_3Cr(CO)_{14}]$ ($[PPN]_2$[1b]). *Method A.* MeOH (15 mL)/MeCN (5 mL) was added to a mixture of $[PPN][Se_2Mn_3(CO)_9]$ (0.86 g, 0.77 mmol), $Cr(CO)_6$ (0.34 g, 1.55 mmol), PPNCl (0.81 g, 1.41 mmol), and KOH (4.48 g, 80 mmol) in an ice−water bath. The mixture was stirred at room temperature for 17 h. The solid was collected by filtration, washed with deionized water and MeOH, and then extracted with CH_2Cl_2, which was recrystallized with CH_2Cl_2/MeOH/Et_2O to give a reddish-brown sample of $[PPN]_2[HSe_2Mn_3Cr(CO)_{14}]$ ($[PPN]_2$[**1b**]) (0.63 g, 0.34 mmol) (yield: 44% based on $[PPN][Se_2Mn_3(CO)_9]$). IR (ν_{CO}, CH_2Cl_2): 2050 (w), 1964 (vs), 1958 (vs), 1930 (w), 1891 (m), 1866 (m) cm^{-1}. ^1H NMR (400 MHz, DMSO-d_6, 300 K): δ −7.78 (s, hydride) (chemical shifts not given for $[PPN]^+$). Anal. Calcd for $[PPh_4]_2$[**1b**]: C, 51.48; H, 2.86. Found: C, 51.39; H, 2.89. Crystals of $[PPh_4]_2$[**1b**] suitable for X-ray diffraction were grown from CH_2Cl_2/MeOH/Et_2O. ICP-AES: Mn:Cr = 3.06:1.

Similar procedures were applied for the preparation of $[TMBA]_2[HSe_2Mn_3Cr(CO)_{14}]$ by using $[TMBA][Se_2Mn_3(CO)_9]$ (0.75 g, 1.04 mmol), $Cr(CO)_6$ (0.50 g, 2.27 mmol), TMBACl (0.85 g, 4.63 mmol), and KOH (4.50 g, 80 mmol) in MeOH (15 mL)/MeCN (5 mL). The yield was 0.88 g (0.83 mmol) of $[TMBA]_2[HSe_2Mn_3Cr(CO)_{14}]$ ($[TMBA]_2$[**1b**]) (80% based on $[TMBA][Se_2Mn_3(CO)_9]$.).

Method B. MeOH (15 mL)/MeCN (5 mL) was added to a mixture of $[PPN][Se_2Mn_3(CO)_9]$ (0.38 g, 0.34 mmol) and $[PPN][HCr(CO)_5]$ (0.50 g, 0.68 mmol) in an ice−water bath. The mixture was stirred at room temperature for 17 h. A methanol solution of PPNCl (0.49 g, 0.85 mmol) was added dropwise to the resulting solution, precipitating the solid. The solid was worked up as above-mentioned to give a reddish-brown sample of $[PPN]_2$[**1b**] (0.19 g, 0.103 mmol) (yield: 30% based on $[PPN][Se_2Mn_3(CO)_9]$).

Synthesis of $[TMBA]_3[S_2Mn_3Cr(CO)_{12}]$ ($[TMBA]_3$[2a]). MeOH (20 mL) was added to a mixture of $[TMBA][S_2Mn_3(CO)_9]$ (0.88 g, 1.40 mmol), $Cr(CO)_6$ (0.31 g, 1.41 mmol), and KOH (4.51 g, 81 mmol). The mixture was stirred at 60 °C for 17 h. A methanol solution of TMBACl (0.91 g, 4.95 mmol) was added dropwise to the resulting solution, precipitating the solid. The solid was collected by filtration, washed with deionized water and MeOH several times, and then extracted with MeCN, which was recrystallized with MeCN/CH_2Cl_2 to give a purplish-black sample of $[TMBA]_3[S_2Mn_3Cr(CO)_{12}]$ ($[TMBA]_3$[**2a**]) (0.93 g, 0.88 mmol) (yield: 63% based on $[TMBA][S_2Mn_3(CO)_9]$). IR (ν_{CO}, MeCN): 1983 (w), 1937 (w), 1904 (vs), 1893 (vs, sh), 1874 (m), 1849 (m), 1790 (vw) cm^{-1}. Anal. Calcd for $[TMBA]_3$[**2a**]·CH_2Cl_2: C, 45.04; H, 3.87; N, 3.66. Found: C, 45.12; H, 4.33; N, 3.62. Crystals of $[TMBA]_3$[**2a**]·CH_2Cl_2 suitable for X-ray diffraction were grown from MeCN/CH_2Cl_2. ICP-AES: Mn:Cr = 2.89:1.

Synthesis of $[TMBA]_3[Se_2Mn_3Cr(CO)_{12}]$ ($[TMBA]_3$[2b]). MeOH (20 mL) was added to a mixture of $[TMBA][Se_2Mn_3(CO)_9]$ (0.50 g, 0.69 mmol), $Cr(CO)_6$ (0.16 g, 0.73 mmol), and KOH (4.57 g, 82 mmol). The mixture was stirred at 60 °C for 24 h. A methanol solution of TMBACl (0.95 g, 5.17 mmol) was added dropwise to the resulting solution, precipitating the solid. The solid was collected by

Table 4. Crystallographic Data for $[PPN]_2[HS_2Mn_3Cr(CO)_{14}]$ ($[PPN]_2$[1a]), $[PPh_4]_2[HSe_2Mn_3Cr(CO)_{14}]$ ($[PPh_4]_2$[1b]), $[TMBA]_3[S_2Mn_3Cr(CO)_{19}]\cdot CH_2Cl_2$ ($[TMBA]_3$[2a]·CH_2Cl_2), $[TMBA]_3[Se_2Mn_3Cr(CO)_{19}]\cdot 0.5CH_2Cl_2$ ($[TMBA]_3$[2b]·$0.5CH_2Cl_2$), $[PPN]_2[HS_2Mn_3Cr_2(CO)_{19}]$ ($[PPN]_2$[3a]), and $[PPN]_2[HSe_2Mn_3Cr_2(CO)_{19}]$ ($[PPN]_2$[3b])

	$[PPN]_2$[**1a**]	$[PPh_4]_2$[**1b**]	$[TMBA]_3$[**2a**]·CH_2Cl_2
empirical formula	$C_{86}H_{61}CrMn_3N_2O_{14}P_4S_2$[a]	$C_{62}H_{41}CrMn_3O_{14}P_2Se_2$	$C_{43}H_{44}Cl_2CrMn_3N_3O_{12}S_2$
fw	1751.19	1446.63	1146.65
cryst syst	triclinic	orthorhombic	triclinic
space group	$P\bar{1}$	*Pbca*	$P\bar{1}$
cryst dimensions			
(mm)	0.38 × 0.34 × 0.08	0.50 × 0.15 × 0.02	0.34 × 0.14 × 0.04
a (Å)	13.6111(6)	19.3174(3)	12.2105(4)
b (Å)	14.6217(7)	24.2509(4)	13.2732(4)
c (Å)	21.674(1)	26.8237(1)	16.8203(6)
α (deg)	88.358(2)		68.679(2)
β (deg)	87.626(2)		85.157(2)
γ (deg)	82.321(2)		88.312(1)
V (Å ^{3})	4269.9(3)	12565.9(3)	2530.5(1)
Z	2	8	2
D_{calcd} ($g\ cm^{-3}$)	1.362	1.529	1.505
μ ($Mo_{K\alpha}$) (mm^{-1})	0.743	2.029	1.188
diffractometer	Nonius (Kappa CCD)	Siemens Smart (Apex CCD)	Nonius (Kappa CCD)
radiation (λ) (Å)	0.71073	0.71073	0.71073
temp (K)	298	298	200
θ range for data collecn (deg)	1.92−24.98	1.52−25.00	1.65−25.02
T_{min}/T_{max}	0.77/0.94	0.55/0.72	0.69/0.95
no. of indep reflns	7898 ($I > 2\ \sigma(I)$)	6562 ($I > 2\ \sigma(I)$)	4983 ($I > 2\ \sigma(I)$)
no. of parameters	1003	761	607
R1[b]/wR2[b]			
($I > 2\ \sigma(I)$)	0.0571/0.1329	0.0554/0.0807	0.0666/0.1562
R1[b]/wR2[b] (all data)	0.1334/0.1843	0.1178/0.0989	0.1198/0.1922

dx.doi.org/10.1021/ic200885h |*Inorg. Chem.* 2011, 50, 7735–7748

Table 4. Continued

	$[TMBA]_3[\mathbf{2b}]\cdot 0.5CH_2Cl_2$	$[PPN]_2[\mathbf{3a}]$	$[PPN]_2[\mathbf{3b}]$
empirical formula	$C_{85}H_{98}Cl_2Cr_2Mn_6N_6O_{24}Se_4$	$C_{91}H_{61}Cr_2Mn_3N_2O_{19}P_4S_2$	$C_{91}H_{61}Cr_2Mn_3N_2O_{19}P_4Se_2$
fw	2408.07	1943.24	2037.04
cryst syst	orthorhombic	triclinic	triclinic
space group	*Pcan*	$P\bar{1}$	$P\bar{1}$
cryst dimensions (mm)	0.43 × 0.4 × 0.2	0.40 × 0.34 × 0.16	0.19 × 0.09 × 0.04
a (Å)	13.2857(1)	14.506(2)	14.344(1)
b (Å)	20.3204(2)	15.018(2)	14.846(1)
c (Å)	35.3790(4)	23.780(3)	23.494(2)
α (deg)		79.726(8)	79.085(4)
β (deg)		83.814(7)	83.113(4)
γ (deg)		64.256(6)	64.752(3)
V (Å ^{3})	9551.3(2)	4588.6(9)	4438.9(6)
Z	4	2	2
D_{calcd} (g cm^{-3})	1.675	1.406	1.524
μ ($Mo_{K\alpha}$) (mm^{-1})	2.639	0.814	1.614
diffractometer	Nonius (Kappa CCD)	Nonius (Kappa CCD)	Nonius (Kappa CCD)
radiation (λ) (Å)	0.71073	0.71073	0.71073
temp (K)	200	298	100
θ range for data collecn (deg)	2.16−25.68	1.64−25.01	1.57−25.03
T_{min}/T_{max}	0.34/0.46	0.74/0.88	0.75/0.94
no. of indep reflns	8819 ($I > 2\sigma(I)$)	5514 ($I > 2\sigma(I)$)	9147
no. of parameters	6940	1099	1096
R1[b]/wR2[b] ($I > 2\sigma(I)$)	0.0402/0.1013	0.1211/0.2948	0.0651/0.1119
R1[b]/wR2[b] (all data)	0.0595/0.1127	0.2791/0.3845	0.1367/0.1346

[a] Water molecule, H_2O, is excluded in the formula, formula weight, calculated density, μ, F(000), and R1/wR2 according to the Platon Squeeze procedure. [b] The functions minimized during least-squares cycles were $R1 = \Sigma||F_o| - |F_c||/\Sigma|F_o|$ and $wR2 = [\Sigma w(F_o^2 - F_c^2)^2/\Sigma w(F_o^2)^2]^{1/2}$.

filtration, washed with deionized water and MeOH several times, and then extracted with MeCN, which was recrystallized with MeCN/CH_2Cl_2 to give a greenish-black sample of $[TMBA]_3[Se_2Mn_3Cr(CO)_{12}]$ ($[TMBA]_3[\mathbf{2b}]$) (0.45 g, 0.39 mmol) (yield: 57% based on $[TMBA][Se_2Mn_3(CO)_9]$). IR (ν_{CO}, MeCN): 1978 (w), 1948 (w), 1905 (vs), 1894 (vs, sh), 1866 (m), 1850 (m), 1782 (vw) cm^{-1}. Anal. Calcd for $[TMBA]_3[\mathbf{2b}]\cdot 0.5CH_2Cl_2$: C, 42.40; H, 4.10; N, 3.49. Found: C, 42.21; H, 3.77; N, 3.49. Crystals of $[TMBA]_3[\mathbf{2b}]\cdot 0.5CH_2Cl_2$ suitable for X-ray diffraction were grown from MeCN/CH_2Cl_2. ICP-AES: Mn:Cr = 2.95:1.

Synthesis of $[PPN]_2[HS_2Mn_3Cr_2(CO)_{19}]$ ($[PPN]_2[\mathbf{3a}]$). CH_2Cl_2 (20 mL) was added to a mixture of $[PPN]_2[\mathbf{1a}]$ (0.20 g, 0.11 mmol) and $Cr(CO)_6$ (0.03 g, 0.14 mmol). The reaction mixture was heated in refluxing CH_2Cl_2 for 12 h. The resulting solution was filtered, and the solvent removed under vacuum. The solid was washed with deionized water and MeOH and then extracted with CH_2Cl_2, which was recrystallized with CH_2Cl_2/MeOH/Et_2O to give a reddish-orange sample of $[PPN]_2[HS_2Mn_3Cr_2(CO)_{19}]$ ($[PPN]_2[\mathbf{3a}]$) (0.12 g, 0.06 mmol) (yield: 55% based on $[PPN]_2[\mathbf{1a}]$). IR (ν_{CO}, CH_2Cl_2): 2054 (w), 1984 (vs), 1979 (vs), 1931 (m), 1905 (w), 1877 (m) cm^{-1}. ^{1}H NMR (400 MHz, DMSO-d_6, 300 K): δ −8.97 (s, hydride) (chemical shifts not given for $[PPN]^+$). Anal. Calcd for $[PPN]_2[\mathbf{3a}]$: C, 56.24; H, 3.16; N, 1.44. Found: C, 56.03; H, 3.04; N, 1.52. Crystals of $[PPN]_2[\mathbf{3a}]$ suitable for X-ray diffraction were grown from CH_2Cl_2/MeOH/Et_2O. ICP-AES: Mn:Cr = 1.51:1.

Synthesis of $[PPN]_2[HSe_2Mn_3Cr_2(CO)_{19}]$ ($[PPN]_2[\mathbf{3b}]$). CH_2Cl_2 (20 mL) was added to a mixture of $[PPN]_2[\mathbf{1b}]$ (0.20 g, 0.11 mmol) and $Cr(CO)_6$ (0.05 g, 0.23 mmol). The reaction mixture was heated in refluxing CH_2Cl_2 for 18 h. The resulting solution was filtered, and the solvent removed under vacuum. The solid was washed with deionized water and MeOH, and then extracted with CH_2Cl_2, which was recrystallized with CH_2Cl_2/MeOH/Et_2O to give a reddish-orange sample of $[PPN]_2[HSe_2Mn_3Cr_2(CO)_{19}]$ ($[PPN]_2[\mathbf{3b}]$) (0.11 g, 0.05 mmol) (yield: 45% based on $[PPN]_2[\mathbf{1b}]$). IR (ν_{CO}, CH_2Cl_2): 2049 (w), 1982 (vs), 1972 (vs), 1931 (m), 1902 (w), 1871 (m) cm^{-1}. ^{1}H NMR (400 MHz, DMSO-d_6, 300 K): δ −7.80 (s, hydride) (chemical shifts not given for $[PPN]^+$). Anal. Calcd for $[PPN]_2[\mathbf{3b}]\cdot$MeOH: C, 53.40; H, 3.17; N, 1.35. Found: C, 53.17; H, 3.45; N, 1.15. Crystals of $[PPN]_2[\mathbf{3b}]$ suitable for X-ray diffraction were grown from CH_2Cl_2/MeOH/Et_2O. ICP-AES: Mn:Cr = 1.68:1.

Conversion of $[TMBA]_2[\mathbf{1a}]$ to $[TMBA]_3[\mathbf{2a}]$. MeOH (20 mL) was added to a mixture of $[TMBA]_2[\mathbf{1a}]$ (1.06 g, 1.09 mmol) and KOH (2.25 g, 40 mmol). The mixture was stirred at 60 °C for 12 h. A methanol solution of TMBACl (0.82 g, 4.46 mmol) was added dropwise to the resulting solution, precipitating the solid. The solid was collected by filtration, washed with deionized water and MeOH several times, and then extracted with MeCN, which was recrystallized with MeCN/CH_2Cl_2 to give a purplish-black sample of $[TMBA]_3[\mathbf{2a}]$ (0.64 g, 0.60 mmol) (yield: 55% based on $[TMBA]_2[\mathbf{1a}]$).

Conversion of $[TMBA]_2[\mathbf{1b}]$ to $[TMBA]_3[\mathbf{2b}]$. MeOH (20 mL) was added to a mixture of $[TMBA]_2[\mathbf{1b}]$ (0.88 g, 0.83 mmol) and KOH (2.25 g, 40 mmol). The mixture was stirred at 60 °C for 14 h. A methanol solution of TMBACl (0.92 g, 5.01 mmol) was added dropwise to the resulting solution, precipitating the solid. The solid was collected by filtration, washed with deionized water and MeOH several times, and then extracted with MeCN, which was recrystallized with MeCN/CH_2Cl_2 to give a greenish-black sample of $[TMBA]_3[\mathbf{2b}]$ (0.40 g, 0.35 mmol) (yield: 42% based on $[TMBA]_2[\mathbf{1b}]$).

dx.doi.org/10.1021/ic200885h |*Inorg. Chem.* 2011, 50, 7735–7748

X-ray Structural Characterization of $[PPN]_2[1a]$, $[PPh_4]_2[1b]$, $[TMBA]_3[2a]\cdot CH_2Cl_2$, $[TMBA]_3[2b]\cdot 0.5CH_2Cl_2$, $[PPN]_2[3a]$, and $[PPN]_2[3b]$. Selected crystallographic data for $[PPN]_2[\mathbf{1a}]$, $[PPh_4]_2[\mathbf{1b}]$, $[TMBA]_3[\mathbf{2a}]\cdot CH_2Cl_2$, $[TMBA]_3[\mathbf{2b}]\cdot 0.5CH_2Cl_2$, $[PPN]_2[\mathbf{3a}]$, and $[PPN]_2[\mathbf{3b}]$ are given in Table 4. All crystals were mounted on glass fibers with epoxy cement. Data collection for $[PPN]_2[\mathbf{1a}]$, $[TMBA]_3[\mathbf{2a}]\cdot CH_2Cl_2$, $[TMBA]_3[\mathbf{2b}]\cdot 0.5CH_2Cl_2$, $[PPN]_2[\mathbf{3a}]$, and $[PPN]_2[\mathbf{3b}]$ was carried out on a Bruker Nonius Kappa CCD diffractometer using graphite-monochromated $Mo_{K\alpha}$ radiation, and an empirical absorption correction by multiscan was applied.[39] Data collection for $[PPh_4]_2[\mathbf{1b}]$ was carried out on a Siemens Smart Apex CCD diffractometer using graphite-monochromated $Mo_{K\alpha}$ radiation employing the $\theta-2\theta$ scan mode, and an empirical absorption correction by multiscan was applied.[39] The structures of $[PPN]_2[\mathbf{1a}]$, $[PPh_4]_2[\mathbf{1b}]$, $[TMBA]_3[\mathbf{2a}]\cdot CH_2Cl_2$, $[TMBA]_3[\mathbf{2b}]\cdot 0.5CH_2Cl_2$, $[PPN]_2[\mathbf{3a}]$, and $[PPN]_2[\mathbf{3b}]$ were solved by direct methods and were refined with SHELXL-97.[40] The hydride atoms of $[PPN]_2[\mathbf{1a}]$, $[PPh_4]_2[\mathbf{1b}]$, $[PPN]_2[\mathbf{3a}]$, and $[PPN]_2[\mathbf{3b}]$ were found in the bridging position across one Mn−Mn bond and were refined with isotropic temperature factors. For $[TMBA]_3[\mathbf{2a}]$, the Mn(1), Mn(2), Mn(3), and Mn(4) atoms and the Cr(1), Cr(2), Cr(3), and Cr(4) atoms of the M_4 square in the two independent forms were with 75 and 25% occupancy, respectively, and were refined with anisotropic temperature factors. For $[TMBA]_3[\mathbf{2b}]$, one independent square M_4 plane showed the disordered M(1) and M(2) atoms with Mn and Cr in 75 and 25% occupancy, and the other one showed the disordered M(3) atom with Mn and Cr present in a 50:50 ratio. All metal atoms were refined with anisotropic temperature factors. For $[PPN]_2[\mathbf{3a}]$, the C(3), O(3); C(4), O(4); C(5), O(5); and C(17), O(17) atoms in the four terminal CO's of the di-$Cr(CO)_5$ group were disordered with 50, 55, 55, and 60% occupancy, respectively, and were refined with isotropic temperature factors. Except for the disordered C and O atoms on the di-$Cr(CO)_5$ group of $[PPN]_2[\mathbf{3a}]$, all of the non-hydrogen atoms for $[PPN]_2[\mathbf{1a}]$, $[PPh_4]_2[\mathbf{1b}]$, $[TMBA]_3[\mathbf{2a}]\cdot CH_2Cl_2$, $[TMBA]_3[\mathbf{2b}]\cdot 0.5CH_2Cl_2$, $[PPN]_2[\mathbf{3a}]$, and $[PPN]_2[\mathbf{3b}]$ were refined with anisotropic temperature factors. The selected distances and angles for $[PPN]_2[\mathbf{1a}]$, $[PPh_4]_2[\mathbf{1b}]$, $[TMBA]_3[\mathbf{2a}]\cdot CH_2Cl_2$, $[TMBA]_3[\mathbf{2b}]\cdot 0.5CH_2Cl_2$, $[PPN]_2[\mathbf{3a}]$, and $[PPN]_2[\mathbf{3b}]$ are listed in Supporting Information, Table S5. Additional crystallographic data are available as CIF files in the Supporting Information.

Electrochemical Measurements. The cyclic voltammetry measurements were performed at room temperature under a nitrogen atmosphere and recorded using a BAS-100W and a CHI 621D electrochemical potentiostat. A platinum working electrode, a platinum wire auxiliary electrode, and a nonaqueous Ag/Ag^+ electrode were used in a three-electrode configuration. Tetra-*n*-butylammonium perchlorate (TBAP) was used as the supporting electrolyte, and the solute concentration was $\sim 10^{-3}-10^{-4}$ M. The redox potentials were calibrated with a ferrocenium/ferrocene (Fc^+/Fc) couple in the working solution and referenced to SCE.

Computational Details. All calculations reported in the present study were performed via the density functional theory (DFT) with Becke's 1988 exchange functional (B) and Perdew's 1986 gradient correlation functional (BP86)[26,27] or Becke's three-parameter (B3) exchange functional and the Lee−Yang−Parr (LYP) correlation functional (B3LYP)[28,29] with a larger basis set: TZVP[30] (triple-ζ valence with one polarization function on each atom) using the Gaussian 03 series of packages.[41] We focused our analyses on the pure DFT method (BP86) because of a better correlation with experimental structural parameters (Supporting Information, Table S4). The geometries of $[E_2Mn_3(CO)_9]^-$ (E = S, Se), **1a**, **1b**, **2a**, **2b**, **3a**, and **3b** were fully optimized using the BP86/TZVP method. Wiberg bond indices[34] and natural charges[35] were evaluated with Weinhold's NBO method.[42] Graphical representations of the molecular orbitals were obtained using CS Chem3D 5.0. For orbital contributions, the molecular orbital compositions were analyzed using the AOMIX program.[43]

■ ASSOCIATED CONTENT

Supporting Information. X-ray crystallographic files in CIF format for $[PPN]_2[\mathbf{1a}]$, $[PPh_4]_2[\mathbf{1b}]$, $[TMBA]_3[\mathbf{2a}]\cdot CH_2Cl_2$, $[TMBA]_3[\mathbf{2b}]\cdot 0.5CH_2Cl_2$, $[PPN]_2[\mathbf{3a}]$, and $[PPN]_2[\mathbf{3b}]$, computational details for the optimized geometries of $[E_2Mn_3(CO)_9]^-$ (E = S, Se), **1a**, **1b**, **2a**, **2b**, **3a**, and **3b**, ORTEPs for **1a**−**3a**, and electrochemical data. This material is available free of charge via the Internet at http://pubs.acs.org.

■ AUTHOR INFORMATION

Corresponding Author
*E-mail: mshieh@ntnu.edu.tw.

■ ACKNOWLEDGMENT

This work was supported by the National Science Council of Taiwan (NSC Grant 98-2113-M-003-006-MY3 to M.S.). We are also grateful to the National Center for High-Performance Computing, which provided the Gaussian package and computer time. Our gratitude also goes to the Academic Paper Editing Clinic, NTNU.

■ REFERENCES

(1) (a) Braunstein, P., Rosé, J. In *Catalysis by Di- and Polynuclear Metal Cluster Complexes*; Adams, R. D., Cotton, F. A., Eds.; Wiley-VCH: New York, 1998; Chapter 13, pp 443−508. (b) Braunstein, P., Rosé, J. *Metal Clusters in Chemistry*; Braunstein, P., Oro, L. A., Raithby, P. R., Eds.; Wiley-VCH: Weinheim, Germany, 1999; Vol. 2, Chapter 2.2, pp 616−677. (c) *Comprehensive Organometallic Chemistry II*; Abel, E. W., Stone, F. G. A., Wilkinson, G., Eds.; *Heteronuclear Metal-Metal Bonds*; Adams, R. D., Ed.; Elsevier: Oxford, 1995; Vol. 10. (d) Sinfelt, J. H. *Bimetallic Catalysts. Discoveries, Concepts and Applications*; Wiley: New York, 1983. (e) *Metal Clusters in Catalysis*; Gates, B. C., Guczi, L., Knözinger, H., Eds.; *Studies in Surface Science and Catalysis Series*; Elsevier: Amsterdam, The Netherlands, 1986; Vol. 29. (f) Hermans, S., Khimyak, T., Raja, R., Sankar, G., Thomas, J. M., Johnson, B. F. G. In *Nanotechnology in Catalysis*; Zhou, B., Hermans, S., Somorjai, G. A., Eds.; Kluwer Academic, Plenum Publishers: New York, 2004.

(2) (a) Thomas, J. M.; Johnson, B. F. G.; Raja, R.; Sankar, G.; Midgley, P. A. *Acc. Chem. Res.* **2003**, *36*, 20–30. (b) Sivaramakrishna, A.; Clayton, H. S.; Makhubela, B. C. E.; Moss, J. R. *Coord. Chem. Rev.* **2008**, *252*, 1460–1485. (c) Adams, R. D.; Captain, B. *Acc. Chem. Res.* **2009**, *42*, 409–418. (d) Adams, R. D.; Captain, B. *Angew. Chem., Int. Ed.* **2008**, *47*, 252–257. (e) Braunschweig, H.; Cogswell, P.; Schwab, K. *Coord. Chem. Rev.* **2011**, *255*, 101–117.

(3) (a) Kahn, O. *Molecular Magnetism*; VCH: Weinheim, Germany, 1993. (b) Mathonière, C., Sutter, J.-P., Yakhmi, J. V. Bimetallic magnets: Present and perspectives. In *Magnetism: molecules to materials*; Miller, J. S., Drillon, M., Eds.; Wiley-VCH: Weinheim, Germany, 2002; Vol. 4.

(4) (a) Robinson, I.; Zacchini, S.; Tung, L. D.; Maenosono, S.; Thanh, N. T. K. *Chem. Mater.* **2009**, *21*, 3021–3026. (b) Femoni, C.; Iapalucci, M. C.; Longoni, G.; Wolowska, J.; Zacchini, S.; Zanello, P.; Fedi, S.; Riccò, M.; Pontiroli, D.; Mazzani, M. *J. Am. Chem. Soc.* **2010**, *132*, 2919–2927. (c) Riccò, M.; Shiroka, T.; Carretta, S.; Bolzoni, F.; Femoni, C.; Iapalucci, M. C.; Longoni, G. *Chem.—Eur. J.* **2005**, *11*, 2856–2861. (d) Eichhöfer, A.; Olkowska-Oetzel, J.; Fenske, D.; Fink, K.; Mereacre, V.; Powell, A. K.; Buth, G. *Inorg. Chem.* **2009**, *48*, 8977–8984. (e) Muratsugu, S.; Sodeyama, K.; Kitamura, F.; Sugimoto, M.; Tsuneyuki, S.; Miyashita, S.; Kato, T.; Nishihara, H. *J. Am. Chem. Soc.* **2009**, *131*, 1388–1389. (f) Costa, M.; Della Pergola, R.; Fumagalli, A.; Laschi, F.; Losi, S.; Macchi, P.; Sironi, A.; Zanello, P. *Inorg. Chem.* **2007**, *46*, 552–560. (g) Prinz, M.; Kuepper, K.; Taubitz, C.; Raekers, M.; Khanra, S.; Biswas, B.; Weyhermüller, T.; Uhlarz, M.;

Wosnitza, J.; Schnack, J.; Postnikov, A. V.; Schröder, C.; George, S. J.; Neumann, M.; Chaudhuri, P. *Inorg. Chem.* **2010**, *49*, 2093–2102. (h) Bechlars, B.; Issac, I.; Feuerhake, R.; Clérac, R.; Fuhr, O.; Fenske, D. *Eur. J. Inorg. Chem.* **2008**, 1632–1644. (i) Shieh, M.; Chung, R.-L.; Yu, C.-H.; Hsu, M.-H.; Ho, C.-H.; Peng, S.-M.; Liu, Y.-H. *Inorg. Chem.* **2003**, *42*, 5477–5479.

(5) (a) Kong, X.-J.; Long, L.-S.; Zheng, Z.; Huang, R.-B.; Zheng, L.-S. *Acc. Chem. Res.* **2010**, *43*, 201–209. (b) Femoni, C.; Iapalucci, M. C.; Kaswalder, F.; Longoni, G.; Zacchini, S. *Coord. Chem. Rev.* **2006**, *250*, 1580–1604. (c) Welsch, S.; Gröger, C.; Sierka, M.; Scheer, M. *Angew. Chem., Int. Ed.* **2011**, *50*, 1435–1438. (d) de Silva, N.; Dahl, L. F. *Inorg. Chem.* **2006**, *45*, 8814–8816. (e) Scheer, M.; Schindler, A.; Merkle, R.; Johnson, B. P.; Linseis, M.; Winter, R.; Anson, C. E.; Virovets, A. V. *J. Am. Chem. Soc.* **2007**, *129*, 13386–13387. (f) Femoni, C.; Iapalucci, M. C.; Longoni, G.; Zacchini, S.; Zarra, S. *J. Am. Chem. Soc.* **2011**, *133*, 2406–2409.

(6) (a) Ferrando, R.; Jellinek, J.; Johnston, R. L. *Chem. Rev.* **2008**, *108*, 845–910. (b) Femoni, C.; Iapalucci, M. C.; Longoni, G.; Tiozzo, C.; Zacchini, S. *Angew. Chem., Int. Ed.* **2008**, *47*, 6666–6669. (c) Naitabdi, A.; Toulemonde, O.; Bucher, J. P.; Rosé, J.; Braunstein, P.; Welter, R.; Drillon, M. *Chem.—Eur. J.* **2008**, *14*, 2355–2362. (d) Schweyer-Tihay, F.; Estournès, C.; Braunstein, P.; Guille, J.; Paillaud, J.-L.; Richard-Plouet, M.; Rosé, J. *Phys. Chem. Chem. Phys.* **2006**, *8*, 4018–4028.

(7) (a) Adams, R. D. In *The Chemistry of Metal Cluster Complexes*; Shriver, H. D., Kaesz, H. D.; Adams, R. D., Eds.; VCH: New York, 1990; Chapter 3, p 121. (b) Roberts, D. A., Geoffroy, G. L. In *Comprehensive Organometallic Chemistry*; Wilkinson, G., Stone, F. G. A., Abel, E. W., Eds.; Pergamon: Oxford, 1982; Vol. 6, Chapter 40, p 763.

(8) (a) Wadepohl, H. *Coord. Chem. Rev.* **1999**, *185−186*, 551–568. (b) Cador, O.; Cattey, H.; Halet, J.-F.; Meier, W.; Mugnier, Y.; Wachter, J.; Saillard, J.-Y.; Zouchoune, B.; Zabel, M. *Inorg. Chem.* **2007**, *46*, 501–509.

(9) (a) Whitmire, K. H. *J. Coord. Chem.* **1988**, *17*, 95–204. (b) Roof, L. C.; Kolis, J. W. *Chem. Rev.* **1993**, *93*, 1037–1080. (c) Mathur, P. *Adv. Organomet. Chem.* **1997**, *41*, 243–314. (d) Ogino, H.; Inomata, S.; Tobiya, H. *Chem. Rev.* **1988**, *98*, 2093–2021. (e) King, R. B.; Bitterwolf, T. E. *Coord. Chem. Rev.* **2000**, *206−207*, 563–579.

(10) (a) Lesch, D. A.; Rauchfuss, T. B. *Inorg. Chem.* **1981**, *20*, 3583–3585. (b) Holliday, R. L.; Roof, L. C.; Hargus, B.; Smith, D. M.; Wood, P. T.; Pennington, W. T.; Kolis, J. W. *Inorg. Chem.* **1995**, *34*, 4392–4401. (c) Drake, G. W.; Schimek, G. L.; Kolis, J. W. *Inorg. Chim. Acta* **1995**, *240*, 63–69. (d) Calderoni, F.; Demartin, F.; Iapalucci, M. C.; Laschi, F.; Longoni, G.; Zanello, P. *Inorg. Chem.* **1996**, *35*, 898–905. (e) Hecht, C.; Herdtweck, E.; Rohrmann, J.; Hermann, W. A.; Beck, W.; Fritz, P. M. *J. Organomet. Chem.* **1987**, *330*, 389–396. (f) Imhof, W.; Huttner, G.; Eber, B.; Günauer, D. *J. Organomet. Chem.* **1992**, *428*, 379–400. (g) Bachman, R. E.; Whitmire, K. H. *Organometallics* **1993**, *12*, 1988–1992. (h) Bachman, R. E.; Whitmire, K. H. *Inorg. Chem.* **1994**, *33*, 2527–2533.

(11) (a) Shieh, M. *J. Cluster Sci.* **1999**, *10*, 3–36. (b) Shieh, M.; Ho, C.-H. *C. R. Chim.* **2005**, *8*, 1838–1849. (c) Lai, Y.-W.; Cherng, J.-J.; Sheu, W.-S.; Lee, G.-A.; Shieh, M. *Organometallics* **2006**, *25*, 184–190.

(12) (a) Adams, R. D.; Kwon, O.-S.; Miao, S. *Acc. Chem. Res.* **2005**, *38*, 183–190. (b) Adams, R. D.; Miao, S. *J. Organomet. Chem.* **2003**, *665*, 43–47. (c) Huang, S. D.; Lai, C. P.; Barnes, C. L. *Angew. Chem., Int. Ed. Engl.* **1997**, *36*, 1854–1856. (d) Fang, Z.-G.; Hor, T. S. A.; Mok, K. F.; Ng, S.-C.; Liu, L.-K.; Wen, Y.-S. *Organometallics* **1993**, *12*, 1009–1011. (e) Alper, H.; Sibtain, F.; Einstein, F. W. B.; Willis, A. C. *Organometallics* **1985**, *4*, 604–606. (f) Ruiz, J.; Ceroni, M.; Quinzani, O. V.; Riera, V.; Vivanco, M.; García-Granda, S.; Van der Maelen, F.; Lanfranchi, M.; Tiripicchio, A. *Chem.—Eur. J.* **2001**, *7*, 4422–4430. (g) Yao, W.-R.; Guo, D.-S.; Liu, Z.-H.; Zhang, Q.-F. *J. Mol. Struct.* **2003**, *657*, 165–175.

(13) (a) Seidel, R.; Schnautz, B.; Henkel, G. *Angew. Chem., Int. Ed. Engl.* **1996**, *35*, 1710–1712. (b) Hermann, W. A.; Hecht, C.; Ziegler, M. L.; Balbach, B. *J. Chem. Soc., Chem. Commun.* **1984**, 686–687. (c) Belletti, D.; Graiff, C.; Pattacini, R.; Predieri, G.; Tiripicchio, A. *Eur. J. Inorg. Chem.* **2004**, 3564–3569. (d) Ruiz, J.; Araúz, R.; Ceroni, M.; Vivanco, M.; Van der Maelen, F.; García-Granda, S. *Organometallics* **2010**, *29*, 3058–3061.

(14) (a) Huang, K.-C.; Tsai, Y.-C.; Lee, G.-H.; Peng, S.-M.; Shieh, M. *Inorg. Chem.* **1997**, *36*, 4421–4425. (b) Shieh, M.; Chen, H.-S.; Yang, H.-Y.; Ueng, C.-H. *Angew. Chem., Int. Ed.* **1999**, *38*, 1252–1254. (c) Shieh, M.; Chen, H.-S.; Yang, H.-Y.; Lin, S.-F.; Ueng, C.-H. *Chem.—Eur. J.* **2001**, *7*, 3152–3158. (d) Shieh, M.; Ho, C.-H.; Sheu, W.-S.; Chen, H.-W. *J. Am. Chem. Soc.* **2010**, *131*, 4032–4033. (e) Ho, C.-H.; Chu, Y.-Y.; Lin, C.-N.; Chen, H.-W.; Huang, C.-Y.; Shieh, M. *Organometallics* **2010**, *29*, 4396–4405.

(15) (a) Hoefler, M.; Tebbe, K.-F.; Veit, H.; Weiler, N. E. *J. Am. Chem. Soc.* **1983**, *105*, 6338–6339. (b) Darensbourg, D. J.; Zalewski, D. J. *Organometallics* **1984**, *3*, 1598–1600. (c) Fischer, R. A.; Kneuper, H.-J.; Herrmann, W. A. *J. Organomet. Chem.* **1987**, *330*, 365–376.

(16) (a) Goh, L. Y. *Coord. Chem. Rev.* **1999**, *185−186*, 257–276. (b) Hausmann, H.; Höfler, M.; Kruck, T.; Zimmermann, H. W. *Chem. Ber.* **1981**, *114*, 975–981. (c) Rohrmann, J.; Herrmann, W. A.; Herdtweck, E.; Riede, J.; Ziegler, M.; Sergeson, G. *Chem. Ber.* **1986**, *119*, 3544–3557. (d) Blacque, O.; Brunner, H.; Kubicki, M. M.; Nuber, B.; Stubenhofer, B.; Watchter, J.; Wrackmeyer, B. *Angew. Chem., Int. Ed. Engl.* **1997**, *36*, 351–353. (e) Stauf, S.; Reisner, C.; Tremel, W. *Chem. Commun.* **1996**, 1749–1750. (f) Song, L.-C.; Cheng, H.-W.; Hu, Q.-M. *Organometallics* **2004**, *23*, 1072–1080.

(17) (a) Shieh, M.; Ho, L.-F.; Guo, Y.-W.; Lin, S.-F.; Lin, Y.-C.; Peng, S.-M.; Liu, Y.-H. *Organometallics* **2003**, *22*, 5020–5026. (b) Shieh, M.; Ho, L.-F.; Chen, P.-C.; Hsu, M.-H.; Chen, H.-L.; Guo, Y.-W.; Pan, Y.-W.; Lin, Y.-C. *Organometallics* **2007**, *26*, 6184–6196. (c) Shieh, M.; Miu, C.-Y. *J. Chin. Chem. Soc.* **2010**, *57*, 956–966.

(18) (a) Pasynskii, A. A.; Eremenko, I. L.; Orazsakhatov, B.; Kalinnikov, V. T.; Aleksandrov, G. G.; Struchkov, Y. T. *J. Organomet. Chem.* **1981**, *216*, 211–221. (b) Pasynskii, A. A.; Eremenko, I. L.; Orazsakhatov, B.; Gasanov, G. S.; Novotortsev, V. M.; Ellert, O. G.; Seifulina, Z. M.; Shklover, V. E.; Struchkov, Y. T. *J. Organomet. Chem.* **1984**, *270*, 53–64. (c) Pasynskii, A. A.; Eremenko, I. L.; Orazsakhatov, B.; Rakitin, Y. V.; Novotortsev, V. M.; Ellert, O. G.; Kalinnikov, V. T.; Aleksandrov, G. G.; Struchkov, Y. T. *J. Organomet. Chem.* **1981**, *214*, 351–365. (d) Pasynskii, A. A.; Skabitski, I. V.; Torubaev, Y. V.; Semenova, N. I.; Novotortsev, V. M.; Ellert, O. G.; Lyssenko, K. A. *J. Organomet. Chem.* **2003**, *671*, 91–100.

(19) (a) Pasynskii, A. A.; Grigoriev, V. N.; Torubaev, Y. V.; Blokhin, A. I.; Shapovalov, S. S.; Dobrokhotova, Z. V.; Novotortsev, V. M. *Russ. Chem. Bull.* **2003**, *52*, 2689–2700. (b) Pasynskii, A. A.; Torubaev, Y. V.; Grigoriev, V. N.; Blokhin, A. I.; Herberhold, M.; Mathur, P. *J. Cluster Sci.* **2009**, *20*, 193–204. (c) Shieh, M.; Lin, C.-N.; Miu, C.-Y.; Hsu, M.-H.; Pan, Y.-W.; Ho, L.-F. *Inorg. Chem.* **2010**, *49*, 8056–8066.

(20) (a) Ma, Y. Q.; Yu, L.; Hu, C. S.; Chen, X.; Li, J.; Wang, H. G.; Miguel, D. *J. Mol. Struct.* **2003**, *650*, 45–48. (b) Ma, Y.-Q.; Yin, N.; Li, J.; Xie, Q.-L.; Miguel, D. *J. Organomet. Chem.* **2004**, *689*, 1949–1955. (c) Alvarez, B.; García-Granda, S.; Jeannin, Y.; Miguel, D.; Miguel, J. A.; Riera, V. *Organometallics* **1991**, *10*, 3005–3007.

(21) (a) Behrens, H.; Weber, R. *Z. Anorg. Allg. Chem.* **1957**, *291*, 122–130. (b) Behrens, H.; Vogl, J. *Chem. Ber.* **1963**, *96*, 2220–2229. (c) Darensbourg, D. J.; Rokicki, A.; Darensbourg, M. Y. *J. Am. Chem. Soc.* **1981**, *103*, 3223–3224. (d) Darensbourg, M. Y.; Slater, S. *J. Am. Chem. Soc.* **1981**, *103*, 5914–5915. (e) Darensbourg, M. Y.; Deaton, J. C. *Inorg. Chem.* **1981**, *20*, 1644–1646. (f) Darensbourg, M. Y.; Bau, R.; Marks, M. W.; Burch, R. R.; Deaton, J. C., Jr.; Slater, S. *J. Am. Chem. Soc.* **1982**, *104*, 6961–6969.

(22) Cauzzi, D.; Graiff, C.; Pattacini, R.; Predieri, G.; Tiripicchio, A.; Kahlal, S.; Saillard, J.-Y. *Eur. J. Inorg. Chem.* **2004**, 1063–1072.

(23) (a) Vergamini, P. J.; Vahrenkamp, H.; Dahl, L. F. *J. Am. Chem. Soc.* **1971**, *93*, 6326–6327. (b) Seyferth, D.; Henderson, R. S.; Fackler, J. P., Jr.; Mazany, A. M. *J. Organomet. Chem.* **1981**, *213*, C21–C25. (c) Adams, R. D.; Captain, B.; Kwon, O.-S.; Miao, S. *Inorg. Chem.* **2003**, *42*, 3356–3365. (d) Adams, R. D.; Horváth, I. T.; Wang, S. *Inorg. Chem.* **1985**, *24*, 1728–1730. (e) Adams, R. D.; Babin, J. E.; Wang, J.-G.; Wu, W. *Inorg. Chem.* **1989**, *28*, 703–709. (f) Brunner, H.; Lucas, D.; Monzon, T.; Mugnier, Y.; Nuber, B.; Stubenhofer, B.; Stückl, A. C.; Wachter, J.; Wanninger, R.; Zabel, M. *Chem.—Eur. J.* **2000**, *6*, 493–503.

(24) (a) Adams, R. D.; Wolfe, T. A.; Wu, W. *Polyhedron* **1991**, *10*, 447–454. (b) Mathur, P.; Hossain, M. M.; Rashid, R. S. *J. Organomet. Chem.* **1994**, *467*, 245–249. (c) Fong, S.-W. A.; Vittal, J. J.; Hor, T. S. A. *Organometallics* **2000**, *19*, 918–924. (d) Belletti, D.; Graiff, C.; Pattacini, R.; Predieri, G.; Tiripicchio, A.; de Biani, F. F.; Zanello, P. *Inorg. Chim. Acta* **2005**, *358*, 161–172.

(25) Ghosh, S.; Kabir, S. E.; Pervin, S.; Hossain, G. M. G.; Haworth, D. T.; Lindeman, S. V.; Siddiquee, T. A.; Bennett, D. W.; Roesky, H. W. *Z. Anorg. Allg. Chem.* **2009**, *635*, 76–87.

(26) Becke, A. D. *Phys. Rev. A* **1988**, *38*, 3098–3100.

(27) Perdew, J. P. *Phys. Rev. B* **1986**, *33*, 8822–8824.

(28) (a) Becke, A. D. *J. Chem. Phys.* **1993**, *98*, 5648–5652. (b) Becke, A. D. *J. Chem. Phys.* **1992**, *96*, 2155–2160. (c) Becke, A. D. *J. Chem. Phys.* **1992**, *97*, 9173–9177.

(29) Lee, C.; Yang, W.; Parr, R. G. *Phys. Rev. B* **1988**, *37*, 785–789.

(30) Schäfer, A.; Huber, C.; Ahlrichs, R. *J. Chem. Phys.* **1994**, *100*, 5829–5835.

(31) See especially Furche, F.; Perdew, J. P. *J. Chem. Phys.* **2006**, *124*, 044103–044127.

(32) Wang, H. Y.; Xie, Y.; King, R. B.; Schaefer, H. F. *J. Am. Chem. Soc.* **2005**, *127*, 11646–11651.

(33) Wang, H. Y.; Xie, Y.; King, R. B.; Schaefer, H. F. *J. Am. Chem. Soc.* **2006**, *128*, 11376–11384.

(34) Wiberg, K. B. *Tetrahedron* **1968**, *24*, 1083–1096.

(35) (a) Reed, A. E.; Weinhold, F. *J. Chem. Phys.* **1983**, *78*, 4066–4073. (b) Reed, A. E.; Weinstock, R. B.; Weinhold, F. *J. Chem. Phys.* **1985**, *83*, 735–746.

(36) Bard, A. J., Faulkner, L. R. *Electrochemical Methods; Fundamentals and Applications*, 2nd ed.; John Wiley & Sons: New York, 2001; p 291.

(37) Nakanishi, T.; Murakami, H.; Sagara, T.; Nakashima, N. *J. Phy. Chem. B* **1999**, *103*, 304–308.

(38) Shriver, D. F., Drezdon, M. A. *The Manipulation of Air-Sensitive Compounds*; Wiley-VCH Publishers: New York, 1986.

(39) Blessing, R. H. *Acta Crystallogr., Sect. A* **1995**, *51*, 33–38.

(40) Sheldrick, G. M. *SHELXL97*, version 97-2; University of Göttingen: Göttingen, Germany, 1997.

(41) Frisch, M. J.; Trucks, G. W.; Schlegel, H. B.; Scuseria, G. E.; Robb, M. A.; Cheeseman, J. R.; Montgomery, J. A., Jr.; Vreven, T.; Kudin, K. N.; Burant, J. C.; Millam, J. M.; Iyengar, S. S.; Tomasi, J.; Barone, V.; Mennucci, B.; Cossi, M.; Scalmani, G.; Rega, N.; Petersson, G. A.; Nakatsuji, H.; Hada, M.; Ehara, M.; Toyota, K.; Fukuda, R.; Hasegawa, J.; Ishida, M.; Nakajima, T.; Honda, Y.; Kitao, O.; Nakai, H.; Klene, M.; Li, X.; Knox, J. E.; Hratchian, H. P.; Cross, J. B.; Bakken, V.; Adamo, C.; Jaramillo, J.; Gomperts, R.; Stratmann, R. E.; Yazyev, O.; Austin, A. J.; Cammi, R.; Pomelli, C.; Ochterski, J. W.; Ayala, P. Y.; Morokuma, K.; Voth, G. A.; Salvador, P.; Dannenberg, J. J.; Zakrzewski, V. G.; Dapprich, S.; Daniels, A. D.; Strain, M. C.; Farkas, O.; Malick, D. K.; Rabuck, A. D.; Raghavachari, K.; Foresman, J. B.; Ortiz, J. V.; Cui, Q.; Baboul, A. G.; Clifford, S.; Cioslowski, J.; Stefanov, B. B.; Liu, G.; Liashenko, A.; Piskorz, P.; Komaromi, I.; Martin, R. L.; Fox, D. J.; Keith, T.; Al-Laham, M. A.; Peng, C. Y.; Nanayakkara, A.; Challacombe, M.; Gill, P. M. W.; Johnson, B.; Chen, W.; Wong, M. W.; Gonzalez, C.; Pople, J. A. *Gaussian 03*, Revision E.04; Gaussian, Inc.: Wallingford, CT, 2004.

(42) Reed, A. E.; Curtiss, L. A.; Weinhold, F. *Chem. Rev.* **1988**, *88*, 899–926.

(43) Gorelsky, S. I. *AOMix program*; http://www.sg-chem.net/.